論文 / 著書情報
Article / Book Information

題目(和文)	
Title(English)	Analysis on the Mechanism of Surface Roughness Development in Melt Spinning of Blend Fibers for Artificial Hair
著者(和文)	徐暁師
Author(English)	XiaoShi Xu
出典(和文)	学位:博士(工学), 学位授与機関:東京工業大学, 報告番号:甲第9281号, 授与年月日:2013年9月25日, 学位の種別:課程博士, 審査員:鞠谷 雄士,扇澤 敏明,森川 淳子,塩谷 正俊,淺井 茂雄
Citation(English)	Degree:Doctor (Engineering), Conferring organization: Tokyo Institute of Technology, Report number:甲第9281号, Conferred date:2013/9/25, Degree Type:Course doctor, Examiner:,,,,
学位種別(和文)	博士論文
Type(English)	Doctoral Thesis

Acknowledgements

This dissertation is based on the research carried out under the guidance of Professor Kikutani in the department of Organic and Polymeric Materials, Tokyo Institute of Technology, Japan, from October, 2008 to July, 2013.

First and foremost, I am most grateful to my supervisor, Professor Kikutani, whose useful suggestions, incisive comments and constructive criticisms have contributed greatly to the completion of this thesis. He devoted a considerable portion of his time to read my manuscripts and make suggestions for the further revisions. I also feel quite appreciate for his care for my daily life in Japan.

I am also greatly indebted to all my teachers who have helped me directly and indirectly in my studies. Especially, Dr.Takarada who directed me to figure out so many problems in the research process. I also want to thank Mr. Shirakashi and Dr. Ishibashi, as my partner he gave me lots of genuine opinions and help. Thanks are also given to all the members in Kikutani laboratory, thanks for their help in melt spinning experiments. I also acknowledge all of the friendly Japanese people, especially my Japanese teacher Mr. Sasaki.

Finally, heartily thank my parents for their selfless devotion. During these five years, I couldn't stay with them as their only daughter, however I can feel their blessing and supporting at any moment.

Xiaoshi Xu
Kikutani Laboratory
Department of Organic and Polymeric Materials
Graduate School of Science and Engineering
Tokyo Institute of Technology
Tokyo, Japan
July, 2013

Contents

Chapter1

General Introduction…...…….....1

1.1 Introduction of Rough Surface Natural Fibers……..……....2

1.2 Introduction Artificial Hair Industry……..…….……...2

1.3 Contents of the Thesis……...…….....4

Reference…….……6

Chapter 2

Formation Conditions for Development of Roughness in Melt Spinning with Polymer Blends ….....9

2.1 Introduction…….10

2.2Experimental…….10

2.2.1 Materials and Melt Spinning Conditions…..……10

2.2.2 Scanning Electron Microscope…….12

2.3 Results and Discussion……....12

2.4 Conclusions……..14

Reference……15

Chapter 3

Comparison of Equipment for Quantitative Evaluation of Surface Roughness of Blend Fibers………22

3.1 Introduction…….....23

3.2 Experimental……24

3.2.1 Materials and Melt Spinning Conditions…..…….……...24

3.2.2 Scanning Electron Microscope…….24

3.2.3 Optical Microscope …….....24

3.2.4 Back Illumination type Diameter monitor ……...25

3.2.5 Edge Detection type Diameter Monitor ……...……...25

3.2.6 Evaluation of surface roughness……...26

3.3 Results and Discussion……27

3.3.1 Off-line measurement of surface roughness…….27

3.3.2 Comparison of on-line and off-line measurements……..27

3.3.3 On-line measurement of spin-line diameter at various positions.29

3.4 Conclusions……....……..31

Reference...……...……..32

Chapter 4

Influence of Various Spinning Conditions on Surface Roughness Development in Melt spinning of PA6/PET Blend Fibers for Artificial Hair……...…..……45

4.1 Introduction……46

4.2 Experimental…….....46

4.2.1 Materials and Melt Spinning Conditions…..……46

4.2.2 Scanning Electron Microscope……47
4.2.3 Edge Detection type Diameter Monitor…….....47
4.2.4Wide Angle X-ray Diffraction……...47
4.2.5 Differential Scanning Calorimetry…….....48
4.2.6 High Speed Camera……..48
4.3 Results and Discussion…….....48
4.3.1 Effect of Extrusion Temperature…….……48
4.3.2 Effect of Nozzle Diameter ……...…….....49
4.3.3 Effect of Through-put Rate…….……..……..50
4.3.4 Effect of Take-up Velocity…..…….50
4.3.5 Effect of Water Bath…….……51
4.3.6 Effect of the Intrinsic Viscosity of PET Component……51
4.4 Conclusions.....….....52
Reference……53

Chapter 5

Mechanism of Surface Roughness Development in Melt Spinning of PA6/PET Blend Fibers for Artificial Hair

……...……65
5.1 Introduction……66
5.2 Experimental…….....66
5.2.1 Materials and Melt Spinning Conditions…..……66
5.2.2 Scanning Electron Microscope…….67
5.2.3 Edge Detection type Diameter Monitor…….....67
5.2.4 Wide Angle X-ray Diffraction……..67
5.2.5 Differential Scanning Calorimetry…….....68

5.2.6 Laser Microscope……...……..68
5.2.7 Acid Treatment of Blend Fiber…….……..……..68
5.3 Results and Discussion…….....68
5.3.1 Crystallization of PET Component of Rough and Smooth Surface PA6/PET Blend Fibers……68
5.3.2 Crystallization of PET Component of Rough and Smooth Surface co-PA/PET/PET Blend Fiber……..……71
5.3.3 Effect of Temperatures of Barrel, Adapter, etc…….…....73
5.3.4 Development of Roughness along the Spin-line…….....74
5.3.5 Differentiation of PET Component in PA6/PET Blend Fiber…..74
5.4 Conclusions.....….....75
Reference……77

Chapter 6

General Conclusions……95

List of publications……..99
Scientific Presentations……100

Chapter1

General introduction

1.1 Introduction of rough surface natural fiber

1.2 Introduction of artificial hair industry

1.3 Contents of the thesis

Reference

Chapter1

General Introduction

1.1 Introduction of rough surface fiber

There are various kinds of natural fibers, i.e. cotton, wool, jute, feather etc. Human beings favor the products made of natural fibers because of their better performance: good air-permeability, appropriate glossiness and low irritation to skin. [1] Natural fibers' specificity makes them not easily be replaced with the artificial fibers. Furthermore, both the principal components and growth processes of natural fibers are difficult to be imitated in the fiber and textile industries.

Animal fibers are very important components of natural fibers. Surfaces of animal fibers are mostly uneven as shown in Figure1-1. The SEM picture of human hair is shown in Figure1-2, and the SEM picture of ordinary synthetic fiber is shown in Figure1-3. The visual contrast of natural fibers and synthetic fibers is remarkable. The roughness on the surface of animal and human hair can influence the glossiness, friction coefficient and air-permeability.

1.2 Introduction of artificial hair industry

Human hair wig has very long history. In China, at least early in B.C. 256, hairpieces were used as daily ornaments by women [2]. In ancient European palace, hairpieces were also regarded as indispensable ornaments. For a very long period, the hairpieces had been produced using natural fibers such as human hair or animal hairs. In the modern times, there are a large number of bald-headed persons all over the world, since the baldness can be caused by high spirit pressure and unhealthy living style. [3] Naturally, there are various remedial measures, however the use of hairpieces has been widely accepted as the most secure and convenient method to cover the baldness. Until

now, hairpieces were made by both human hair and artificial hair. Since human hair is not easy to obtain and care, the application of synthetic fiber is becoming the most popular method. As stated previously, surface roughness is one of the most important characteristics of natural fibers and animal hairs. Therefore, in order to produce advanced hairpiece with synthetic fiber, control of surface roughness is indispensable for achieving satisfactory appearance.

In terms of the technological development in fiber industry, there are mainly three industrial technologies for formation of rough surface fibers: Firstly enhancement of the formation of spherullites in the melt spinning of polyamide fibers was utilized [4] as shown in Figure 1-4. In this process, polyamide 6 or polyamide 66 filament extruded from the spinneret was passed through a water bath to reduce cooling speed. Temperature of the bath was 30 – 80 ^{o}C. It was concluded that there was an enhancement of roughness development with the increase of the bath length. It was also reported that the fibers with surface roughness can be produced through the extraction of soluble component after formation of blend fibers [5] as shown in Figure 1-5. In this process, fibers were prepared using polyamide 6 blended with alkali-soluble co-polyester containing 1 – 40 wt% of inorganic powder. The rough surface fibers were produced by treating the fibers with 5 wt% aqueous solution of sodium hydroxide at 95 ^{o}C for 4 hours. The most recent technology in this field is the erosion of fiber surface by sand-blasting [6] as shown in Figure 1-6. It was reported that multiple polyamide filaments can be treated simultaneously at the moving speed of 200 – 300 m/min. This means that the melt spinning process and the sand-blasting process can be connected. Sand-blasting of fibers after the formation of spherullites was also proposed.

Even though the appearance of these fibers are good enough for artificial hair applications, there are some disadvantages in these technologies. Formation of spherullites can be achieved only for limited polymers and spinning conditions. Treatment with solution is time- and energy-consuming and harmful to the environment. Sand-blasting requires special equipment. Use of small particles also needs special care

for the working environment. On the other hand, we recently found that the fibers with highly developed surface roughness can be formed in melt spinning of blend fibers under wide-range of spinning conditions. [7] In comparison with the conventional methods, this new method is more flexible in terms of the range of spinning conditions and selection of polymers. With the aim of clarifying the key parameters for the control of surface roughness, effect of various spinning conditions on the evolution of surface roughness and mechanism of surface roughness development were investigated in this research.

1.3 Contents of the Thesis

Chapter 1 is the general introduction of this thesis. It was stated that incorporation of surface roughness is necessary in the production of fibers for artificial hair since human hair as well as hair of any animal exhibits surface roughness. Various technologies developed in the artificial hair industry for producing synthetic fibers with surface roughness was introduced.

In chapter 2, we found that fibers with highly developed surface roughness can be formed in the melt spinning of polyamide 6 (PA6)/poly(ethylene terephthalate) (PET) blend fibers under certain spinning conditions. To elucidate the necessary conditions for the development of roughness on the fiber surface, melt spinning of various combinations of blend polymers was carried out under a wide-range of spinning conditions. Materials and necessary spinning conditions for formation of rough surface fibers were clarified.

In chapter 3, three kinds of optical equipment including edge detection type diameter monitor (EDDM), back illumination type diameter monitor (BIDM) and optical microscope (OM) were applied for the quantitative evaluation of the surface roughness of PA6/PET blend fibers. There was a good correlation between the roughness values evaluated using the edge detection type diameter monitor (EDDM)

and the back-illumination type diameter monitor (BIDM), even though resolution of the BIDM is lower than that of the EDDM. Through the on-line measurement of spin-line diameter performed at various positions along the spin-line using the BIDM, it was revealed that the development of surface roughness proceeds with the increase of distance from the spinneret.

In chapter 4, rough surface blend PA6/PET fibers spun with different spinning temperatures, nozzle diameters, through-put rates and take-up velocities were compared. The influences of cooling method and intrinsic viscosity of PET component were also investigated. Roughness of these fibers was measured by the edge-detection type diameter monitor (EDDM) and the scanning electron microscope (SEM), formation of fibers was observed by a high speed camera (HSC), crystallization of PA6/PET fibers spun with different spinning conditions was analyzed by differential scanning calorimetry (DSC) measurement and wide angle X-ray diffraction (WAXD) measurement.

In chapter 5, barrel temperatures were changed to investigate further the formation process of roughness during melt spinning. The results of differential scanning calorimetry (DSC) measurement and wide angle X-ray diffraction (WAXD) measurement revealed the change in the crystallizability of PET component in PA6/PET and co-PA/PET blend fibers spun with various conditions. A scanning electron microscope study with energy dispersive X-ray detector-analysis (SEM-X) and the surface treatment technique of fibers with alkali were applied for the differentiation of PA6 and PET components in the blend fibers.

In Chapter 6, major conclusions obtained in the above chapters are summarized.

Reference

[1] Fibers and basic knowledge of fabric, Editor：Tokyo Metropolitan Industrial Technology Research Institute（2010）

[2] Xu Hongquan, Journal of Literature and History, 3, 70-71(2000)

[3] José M. Martín MD, Carlos Monteagudo MD, Encarnación Montesinos MD, Jorge Guijarro MD, Beatriz Llombart MD, American Academy of Dermatology, 52, 152-156(2005)

[4] Shirakashi Yutaka, Production method for artificial hair, JP 62-156308, 1995

[5] Ono Yosuke, Production method for artificial hair by using synthetic fibers, JP 2007-303014

[6] Shirakashi Yutaka, Production method for artificial hair, JP 2003-239128, 2003

[7] Xu X, Shirakashi Y, Ishibashi J, Takarada W, Kikutani T., Analysis on the Development of Surface Roughness in Melt Spinning of Fibers for Artificial Hair. ATC-10: Proceeding of Asian Textile Conference; 2009 Sep 7-9; Ueda, Nagano, Japan.

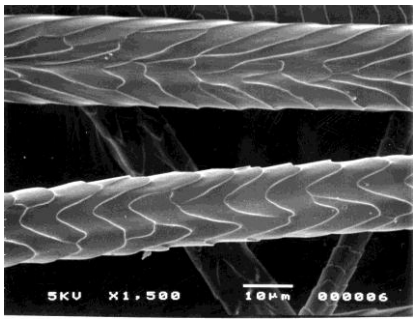

Rabbit

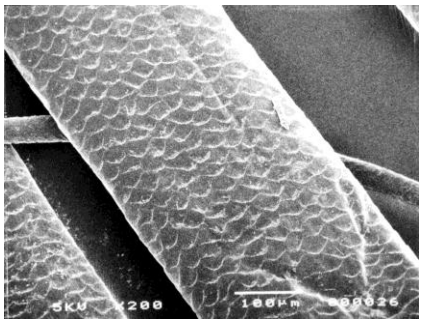

Reindeer

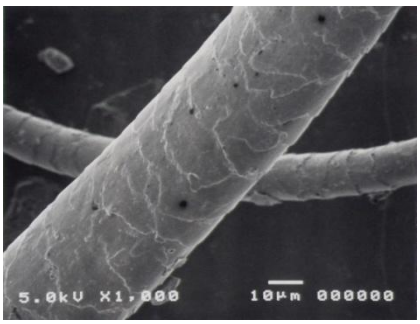

Yak

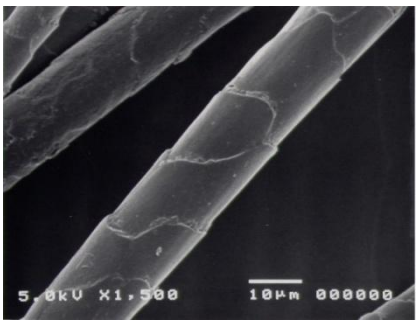

Wool

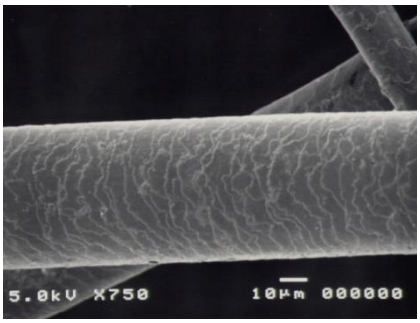

Alpaca

Figure 1-1. SEM pictures of animal hair (Picture were supplied by Tokyo Metropolitan Industrial Technology Research Institute).

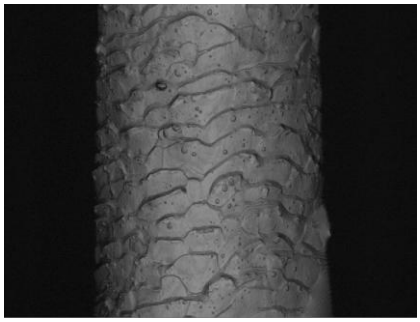

Figure 1-2. Laser microscope photograph of Human hair.

Figure 1-3. SEM photograph of smooth surface synthetic fiber produced by melt spinning.

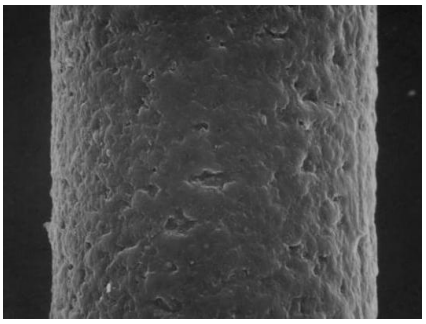

Figure 1-4. SEM photograph of rough surface synthetic fiber produced by the sand-blasting method.

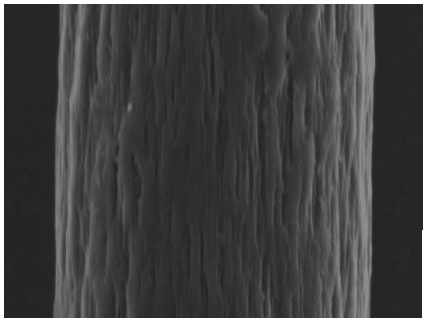

Figure 1-5. SEM photograph of rough surface synthetic fiber produced by the method of extracting soluble component.

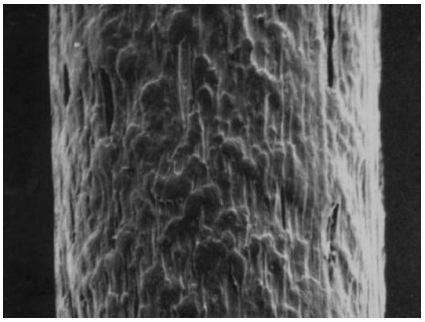

Figure 1-6. SEM photograph of rough surface synthetic fiber produced by the method of enhancing the formation of spherullites.

Chapter 2

Formation Conditions for Development of Roughness in Melt Spinning with Polymer Blends

2.1 Introduction

2.2 Experimental

2.2.1 Materials and Melt Spinning Conditions

2.2.2 Scanning Electron Microscope

2.2.3Wide Angle X-ray Diffraction

2.2.4Differential Scanning Calorimetry

2.3 Results and Discussion

Conclusions

Reference

Chapter2

General Introduction

Formation Conditions for Roughness in Melt Spinning with Polymer Blends

2.1 Introduction

It has been recognized that the surface roughness is one of the most important characteristics in the production of fibers for artificial hair. It was found that the fibers with highly developed surface roughness can be formed in the melt spinning of polyamide 6 (PA6)/poly (ethylene terephthalate) (PET) blend fibers under certain spinning conditions. To elucidate the necessary conditions for the development of roughness on the fiber surface, melt spinning of various combinations of blend polymers was carried out under a wide-range of spinning conditions in this chapter.

2.2 Experiment

2.2.1 Materials and Spinning Conditions

The materials applied in this chapter were polyamide 6 (PA6) (NOVAMID 1020, DSM Japan Engineering Plastics), poly(ethylene terephthalate) (PET) (PETMAX RE530A, TOYOBO Co., Ltd.), amorphous co-polyester (co-PCT) (AN004, Eastman Co., Ltd.), amorphous co-polyamide (co-PA) (NOVAMID X21, DSM Japan Engineering Plastics), poly(butylene terephthalate) (PBT) (PBT 500LP, Polyplastics Co., Ltd.), PBT copolymer (co-PBT) (PBT 600FP, Polyplastics Co., Ltd.) and polypropylene (PP) (Y2000GP, Idemitsu Kosan Co., Ltd.). According to the supplier data sheet, chemical structure formulas of co-PA and co-PCT are represented as follows:

co-PA 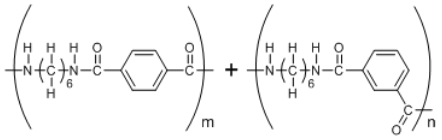

co-PCT 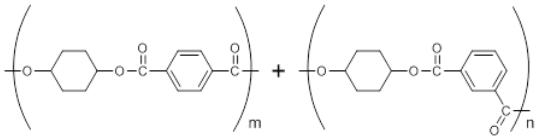

Chemical structure of co-PBT was not disclosed by the producer. However, it was revealed that the melting temperature of the co-PBT is around 170 oC, which is significantly lower than that of pure PBT, 223 ^{o}C. Combinations of major and minor components applied for the melt spinning experiments are summarized in Table 2-1. Composition of major/minor components was fixed at 80/20 wt%. It should be noted that co-PA and co-PCT are amorphous polymers with their glass transition temperatures of 125 and 75 ^{o}C, respectively.

Dry-blended polymer pellets were melted and extruded through a twin screw extruder equipped with a metering pump and a spinneret with single hole spinning nozzle. The extruded filament was taken-up using a winder placed at 2.0 m below the spinneret. Conditions for melt spinning are also shown in Table 1. In that table, barrel temperatures C1 to C4 correspond to the zone temperatures from upstream to downstream in the extruder. In all cases, the highest temperature in the twin screw extruder was set to be higher than the melting temperatures of both components, whereas the extrusion temperature was adjusted in the regions of the metering pump and the spinneret. Through-put rate was controlled to 5.8 g/min. Nozzle diameter was 1.0 or 2.0 mm, and take-up velocity was varied from 124 to 500 m/min. In cases of PP/PBT and PP/co-PBT combinations, winding of the fiber was impossible. Accordingly only the free-fall samples were collected.

2.2.2 Scanning Electron Microscope

More detailed shape of resultant fibers was analyzed using scanning electron microscope (SM-200: TOPCON Co., Ltd). Magnification was 500x.

2.3 Results and Discussion

Melt spinning of blend fibers of various combinations of polymers were carried out with the aim of elucidating the rule for the development of surface roughness. Crystallizability and melting temperature of each component were the factors of interest.

Firstly, SEM photographs of the PA6/PET and PA6/co-PCT blend fibers are compared in Figure 2-1. It should be noted that PET is a crystalline semi-aromatic polyester whereas co-PCT is an amorphous semi-aromatic co-polyester. Both PET and co-PCT have similar glass transition temperatures of around 75 ^{o}C. The SEM photographs show that these blend fibers exhibited smooth surface at a high extrusion temperature of 265 ^{o}C. When the extrusion temperature was lowered to 255 ^{o}C, which is lower than the melting temperature of PET, surface roughness was developed for PA6/PET blend fiber whereas the surface of PA6/co-PCT fiber kept its smoothness. From these results, it would be reasonable to surmise that the crystallizability of the minor component is necessary for the development of surface roughness.

Secondly, effect of the crystallizability of the major component was investigated by using the amorphous co-polyamide, co-PA, as the major component. As shown in Figure 2-2, at the extrusion temperature of 255 ^{o}C, both PA6/PET and co-PA/PET blend fibers exhibited smooth surface, whereas roughness appeared on the surface of both blend fibers when extrusion temperature was at and lower than 245 ^{o}C. These results indicate that the crystallizability of the major component is not necessarily required for the development of surface roughness.

Furthermore, comparison of the results for PA6/PET fibers in Figures.2-1 and 2-2

indicate that at the same extrusion temperature, roughness development is suppressed with the change of nozzle diameter from 2.0 mm to 1.0 mm. On the other hand, because the attainable lowest extrusion temperature is lowered, eventually fibers with more enhanced roughness is obtained in the case of smaller nozzle diameter of 1.0 mm. Influence of nozzle diameter on the roughness development will be discussed in detail in the forthcoming paper.

Thirdly, effect of the relation between the melting temperatures of major and minor components is investigated by comparing the results of the melt spinning of PP/PBT and PP/co-PBT blends. Melting temperatures of PP, PBT and co-PBT are about 165, 223 and 170 ^{o}C, respectively. The SEM photographs of PP/PBT and PP/co-PBT fibers are shown in Figure 2-3. There was a development of surface roughness for PP/PBT blend at the extrusion temperature of 210 ^{o}C, which was lower than the melting temperature of PBT. On the contrary, fibers with surface roughness could not be produced in case of the PP/co-PBT blend. It should be noted that the melting temperature of co-PBT is similar to PP, and therefore, extrusion temperature could not be lowered to a temperature below the melting temperature of the minor component, co-PBT.

Results of a series of experiments described above are summarized in Table 2-2. From this table it was elucidated that the necessary conditions for the development of surface roughness are: (1) the minor component needs to be crystallizable, (2) the major component can be either amorphous or crystalline, but needs to be melt processable at a temperature lower than the melting temperature of the minor component, and (3) the extrusion temperature needs to be lower than the melting temperature of the minor component. It is also revealed that under the conditions for the appearance of surface roughness, roughness development is enhanced by lowering the extrusion temperature.

2.4 Conclusions

To elucidate the necessary conditions for the development of roughness on the surface of blend fibers, melt spinning of various combinations of blend polymers were carried out under a wide-range of spinning conditions. It was concluded that the necessary conditions for the formation of surface roughness are: (1) the minor component is a crystalline polymer, (2) the major component is melt processable at a temperature lower than the melting temperature of the minor component and (3) extrusion temperature is lower than the melting temperature of the minor component.

Reference

[1] Shirakashi Y. Production method for artificial hair, Japan patent 62-156308 (1987).

[2] Ono Y. Production method for artificial hair by using synthetic fibers, Japan patent 2007-303014 (2007).

[3] Shirakashi Y. Production method for artificial hair, Japan patent 2003-239128 (2003).

[3] Shirakashi Y, Asakura O, Ito S, Ishibashi J, Xu X, Takarada W, Kikutani T. Development of Polyamide 6 Based Blend Fibers with Surface Roughness for Artificial Hair. Seikei-Kakou 2011; 23: 358-364.

[5] Xu X, Shirakashi Y, Ishibashi J, Takarada W, Kikutani T. Analysis on the Development of Surface Roughness in Melt Spinning of Fibers for Artificial Hair. ATC-10: Proceeding of Asian Textile Conference; 2009 Sep 7-9; Ueda, Nagano, Japan.

[6] Xu X, Shirakashi Y, Ishibashi J, Takarada W, Kikutani T. Analysis on the Development of Surface Roughness in Melt Spinning of Fibers for Artificial Hair. Preprints of Seikei-Kakou Annual Meeting 2011; 215-216.

[7] Ziabicki A, Fundamentals of Fiber Formation. London: John Wiley & Sons, 1976, p.113.

[8] Shimizu, J.; Okui, N.; Kikutani, T., Fine Structure and Physical Properties of Fibers Melt-spun at High Speeds from Various Polymers in High-Speed Fiber Spinning. New York: John Wiley & Sons, 1985, p.429.

[9] Kikutani T, Nakao K, Takarada W, and Ito H. On-line measurement of orientation development in the high-speed melt spinning process. Polymer Engineering & Science 1999; 39: 2349–2357.

[10] Heuvel HM, Huisman R. Effect of winding speed on the physical structure of as-spun poly(ethylene terephthalate) fibers, including orientation-induced crystallization. Journal of Applied Polymer Science 1978; 22: 2229-2243.

[11] Daubeny R de D, Bunn CW, Brown CJ. The Crystal Structure of Polyethylene Terephthalate. Proc Roy Soc 1954; 226: 531-542.

[12] Matsuba G, Zhao Y, Nishida K, Kanaya T., Precursor of shish–kebab in isotactic polystyrene under shear flow. Polymer 2009; 50: 2095-2103.

Table 2-1 Conditions for melt spinning of blend fibers

Exp. No.	Major Component (80 wt%)	Melting Temperature (^oC)	Minor Component (20 wt%)	Melting Temperature (^oC)	Barrel Temperatures				Nozzle Diameter (mm)	Extrusion Temperature (^oC)
					C1 (^oC)	C2 (^oC)	C3 (^oC)	C4 (^oC)		
1	PA6	220	PET	257	160	260	235	235	2.0	250 ~ 265
	PA6	220	co-PET	∆	160	260	235	235	2.0	250 ~ 265
2	PA6	220	PET	257	160	260	235	235	1.0	235 ~ 255
	co-PA	∆	PET	257	160	260	235	235	1.0	235 ~ 255
3	PP	165	PBT	223	160	260	235	235	1.0	210 ~ 240
	PP	165	co-PBT	170	160	260	235	235	1.0	210 ~ 240

∆: Amorphous polymer, PA6: polyamide, co-PA: co-polyamide, PP: polypropylene, PET: poly(ethylene terephthalate), PBT: poly(butylene terephthalate).

Table 2-2 Results of surface roughness development

Exp. No.1	Nozzle Diameter (mm)	Extrusion Temperatures (^{o}C)				Take-up Velocity (m/min)
		250	255	260	265	
PA6/PET	2.0	○	○	△	×	270
PA6/co-PCT	2.0	×	×	×	×	500
Exp. No.2	**Nozzle Diameter (mm)**	**Extrusion Temperatures (^{o}C)**				**Take-up Velocity (m/min)**
		235	240	245	250	255
PA6/PET	1.0	○	○	○	△	×	124
co-PA/PET	1.0	○	○	○	△	×	124
Exp. No.3	**Nozzle Diameter (mm)**	**Extrusion Temperatures (^{o}C)**				**Take-up Velocity (m/min)**
		210	220	230	240	
PP/PBT	1.0	○	○	△	×	*
PP/co-PBT	1.0	×	×	×	×	*

○: Rough surface
△: Intermediate between rough and smooth surfaces
×: Smooth surface
* : Free-fall

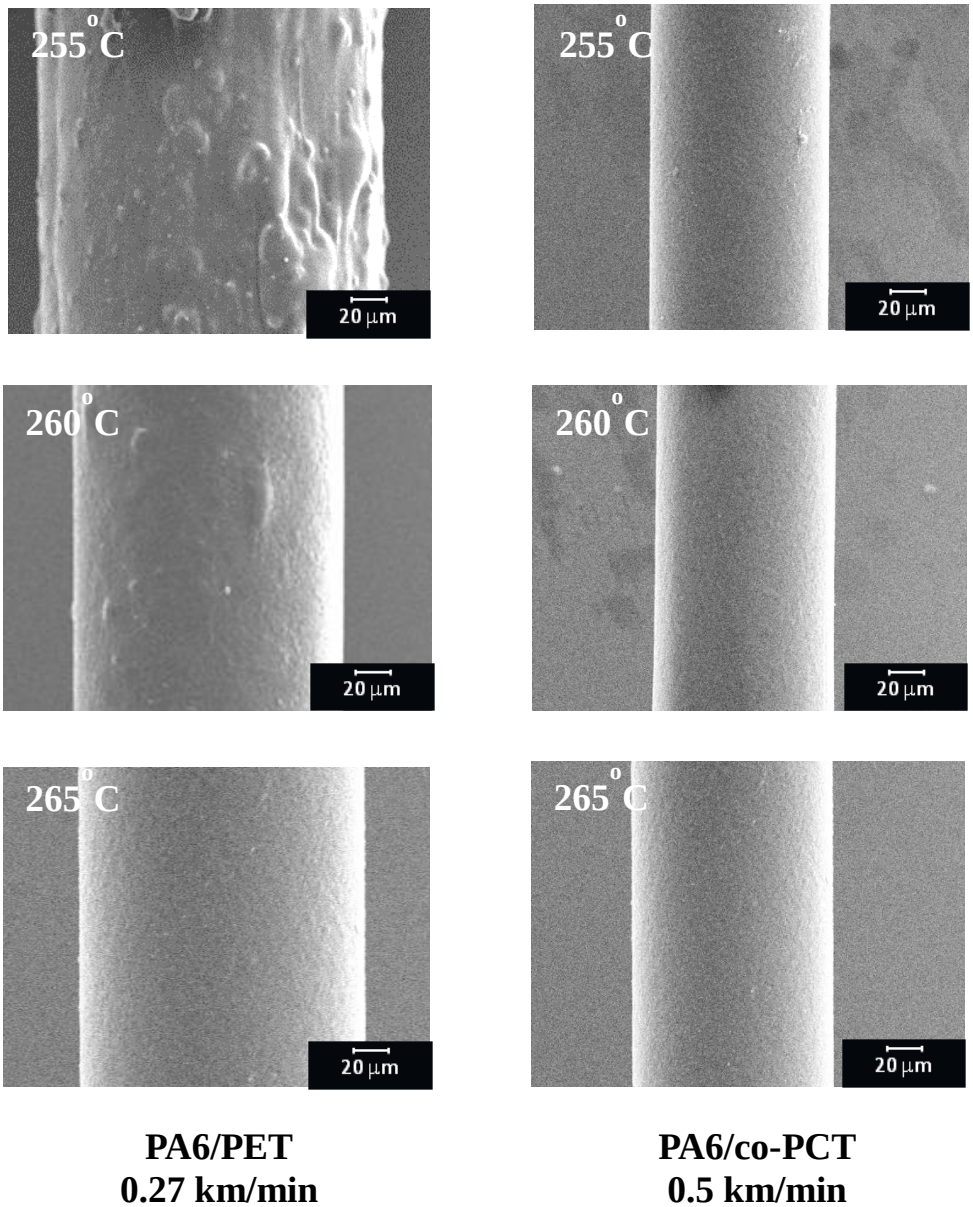

Figure 2-1. SEM photographs of PA6/PET (80/20 wt%) and PA6/co-PCT (80/20 wt%) blend fibers melt-spun with different extrusion temperatures of 255, 260 and 265°C. Through-put rate 5.8 g/min, nozzle diameter 2.0 mm. Take-up velocities for PA6/PET and PA6/co-PCT were 270 and 500 m/min, respectively.

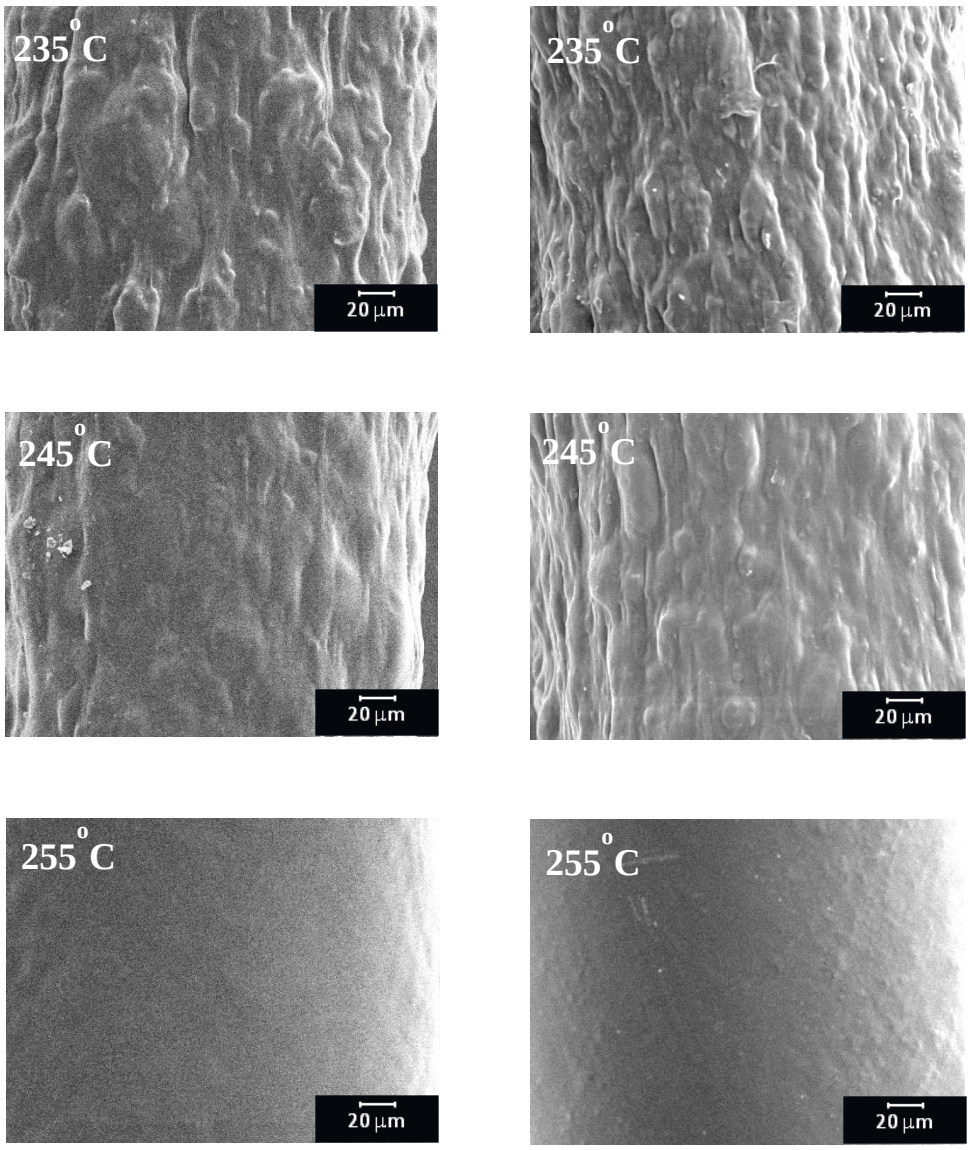

Figure 2-2. SEM photographs of PA6/PET (80/20 wt%) and co-PA/PET (80/20 wt%) blend fibers melt-spun with different extrusion temperatures of 235, 245 and 255 °C. Through-put rate 5.8 g/min, nozzle diameter 1.0 mm, take-up velocity 124 m/min.

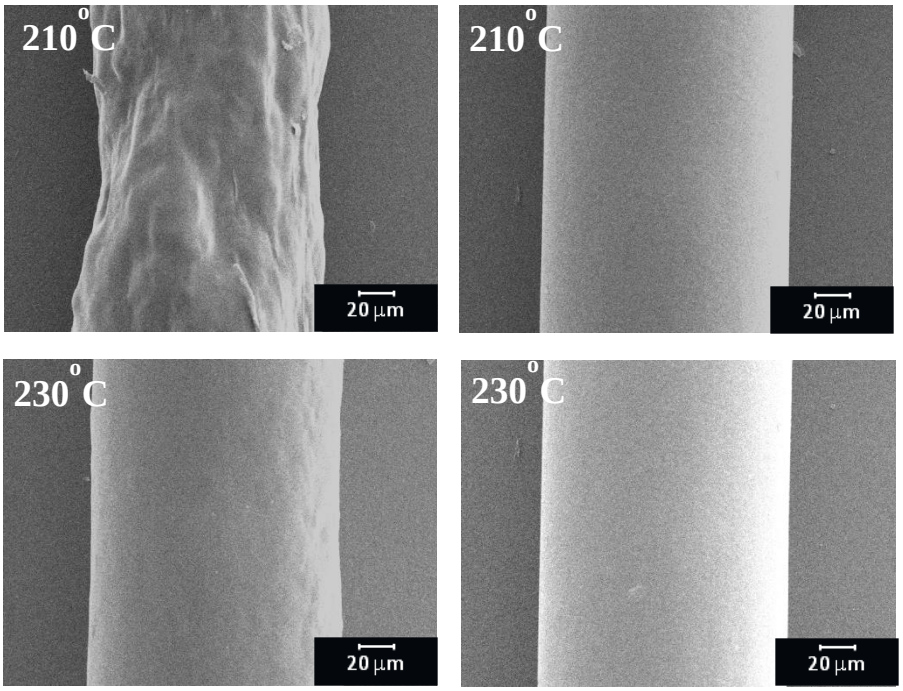

Figure 2-3. SEM photographs of PP/PBT (80/20 wt%) and PP/co-PBT (80/20 wt%) blend fibers melt-spun with different extrusion temperatures of 210 and 230 ^{o}C. Through-put rate 5.8 g/min, nozzle diameter 1.0 mm.

Chapter 3

Comparison of Equipment for Quantitative Evaluation of Surface Roughness of Blend Fibers

3.1 Introduction

3.2 Experimental

3.2.1 Materials and Melt Spinning Conditions

3.2.2 Scanning Electron Microscope

3.2.3 Optical Microscope

3.2.4 Back Illumination type Diameter monitor

3.2.5 Edge Detection type Diameter Monitor

3.2.6 Evaluation of surface roughness

3.3 Results and Discussion

3.3.1 Off-line measurement of surface roughness

3.3.2 Comparison of on-line and off-line measurements

3.3.3 On-line measurement of spin-line diameter at various positions

3.4 Conclusions

Reference

Chapter 3

Comparison of Equipment for Quantitative Evaluation of Surface Roughness of Blend Fibers

3.1 Introduction

Surface roughness is one of the most important characteristics in the production of chemical fibers for artificial hair. Introduction of surface roughness brings about good appearance of fibers similar to human hair such as mild light reflection characteristics, deep color etc. It has been introduced that the fibers with surface roughness of various degrees can be produced through the melt spinning of polyamide 6 (PA6)/poly(ethylene terephthalate) (PET) blend fibers if extrusion temperature is set to be lower than the melting temperature of PET [1,2]. This technology is expected to be applicable for the production of synthetic fibers for artificial hair. Even though characteristics of the surface roughness of prepared fibers were visualized through the observation under a scanning electron microscope (SEM), it was recognized that quantitative analysis of the surface roughness is indispensable. In this chapter, quantitative analysis of the degree of surface roughness was carried out along the fiber axis.

Selection of optical equipment and their measurement methods are the most important points in this research. Except for the use of a SEM and an optical microscope, we also applied a back illumination type diameter monitor (BIDM) and an edge detection type diameter monitor (EDDM). The EDDM has higher positional resolution than the BIDM, whereas the BIDM has the advantage of applicability for the on-line measurement of the thinning behavior of the spin-line during the melt spinning processes [3]. These analyses were found to be useful not only for the quantitative analysis of the roughness on the surface of as-spun fibers but also for clarifying the surface roughness development behavior in the melt spinning process of blend fibers.

3.2 Experimental

3.2.1 Materials and Melt Spinning Conditions

The materials applied in this research were PA6 (NOVAMID 1020, DSM Japan Engineering Plastics) and PET (PETMAX RE530A, Toyobo Co., Ltd.). Dry-blended polymer pellets of PA6 and PET with mass ratio of 80:20 were melted and extruded using an extrusion system consisting of a co-rotating twin-screw extruder with the screw diameter of 15 mm, a gear pump with the capacity of 0.3 cm^3 per revolution and a spinneret with a single-hole nozzle of 0.5 mm diameter. Take-up winder was placed at a position 2.0 m below the spinneret. Through-put rate and take-up velocity were mainly set to 5.8 g/min and 270 m/min, respectively.

More detailed extrusion conditions were as follows. Barrel temperatures C_1 - C_4, i.e. the zone temperatures from upstream to downstream in the extruder, were 160, 260, 235 and 235 ^oC. It should be noted that the highest temperature in the extruder was set to be higher than the melting temperatures of PA6 (220 ^oC) and PET (257 ^oC), whereas the extrusion temperature was adjusted in the region of the gear pump and the spinneret. Extrusion temperatures of 245 and 255 ^oC were mainly adopted to produce as-spun fibers with different degrees of surface roughness. Scanning electron micrographs of the fibers prepared under these conditions are shown in Figure 1. Development of surface roughness could be observed clearly for the fiber extruded at 245 ^oC, whereas the fiber extruded at 255 ^oC exhibited smooth surface.

3.2.2 Scanning Electron Microscope

Surfaces of as-spun fibers were analyzed using a scanning electron microscope (SM-200: TOPCON Co., Ltd) with magnification of 500x. This equipment was only applied for off-line measurement because of its limited measurement area.

3.2.3 Optical Microscope

Rough surface fiber sample of 14 mm long was analyzed by taking pictures under an optical microscope (BH-2: OLYMPUS Co., Ltd). Magnification was 400x. As we all

accepted, OM pictures could show the most accurate details of fiber's surface, but it couldn't be automated. In this measurement, more than 200 photographs of the fiber sample were taken one by one by shifting the position of sample along the fiber axis. The photographs were aligned consecutively to reproduce the "long" fiber image, and then compressed along the fiber axis. Diameter variation along the fiber axis was evaluated for the compressed image using image-analysis software: Photoshop (Adobe Systems Inc.) and Scion Image (Informer Technologies, Inc.).

3.2.4 Back Illumination type Diameter monitor

Back illumination type diameter monitor (BIDM) (Zimmer A/10: Zimmer Japan, Ltd.) was applied as on-line and off-line measurement. In this experiment, evaluation of surface roughness of the fibers was performed through the analysis of fiber diameter variation along the fiber axis. The positional resolution for the direction of fiber axis, maximum sampling rate and effective measurement area are 2.6 mm, 20 kHz and 10 x 11 mm, respectively. Device resolutions for the measurement of fiber diameter are 2.5 μm. In the off-line measurement of as-spun fibers, a single fiber fixed to a cardboard frame was moved along the fiber axis with the speed of 100 mm/min to pass through the measurement areas. Schematic diagram of the measurement system for the analysis of diameter variation of as-spun fibers along the fiber axis is shown in Figure 3-2 (a). As the on-line measurement, BIDM was set at different positions from the spinneret along the spin-line with the conditions of sampling rate of 1 kHz and measurement time at each position of 5 s, see Figure 3-2 (b).

3.2.5 Edge Detection type Diameter Monitor

Edge detection type diameter monitor (EDDM) (LS-7010M: KEYENCE Co., Ltd.) was applied as off-line measurement. The positional resolution for the direction of fiber axis, maximum sampling rate and effective measurement area are 30 μm, 1.2 kHz and 2 x 4

mm, respectively. Device resolutions of EDDM for the measurement of fiber diameter are 0.5 μm. In the off-line measurement of as-spun fibers, the same measurement method was used with the sample rate of 50 Hz, see Figure 3-2 (a). Application of the EDDM for the on-line measurement was difficult since the measurement area of 2 x 4 mm is too small considering the fluctuation of the position of spin-line.

3.2.6 Evaluation of surface roughness

Fiber diameter $D(x)$ measured either as a function of length in the off-line measurement or as a function of time in the on-line measurements showed short range fluctuation caused by the surface roughness as well as long range variation caused by the instability of the spinning process. Therefore, for the evaluation of the degree of short range fluctuation due to the surface roughness, mean value of the deviation of fiber diameter from its moving average over a certain range of length or time, $x_1 \sim x_2$, R_a was calculated using the following equation:

$$R_a = \frac{\int_{x_1}^{x_2} \left| D(x) - \overline{D}(x) \right| dx}{x_2 - x_1} \qquad \text{---- (1)}$$

where $\overline{D(x)}$ is the result of moving average operation for the range of a as expressed in eq. (2).

$$\overline{D}(x) = \frac{\int_{x-a/2}^{x+a/2} D(x)\, dx}{a} \qquad \text{---- (2)}$$

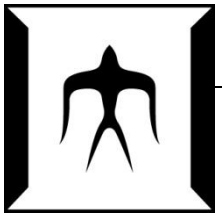

3.3 Results and Discussion

3.3.1 Off-line measurement of surface roughness

As a typical example, results of the off-line measurement of diameter fluctuation for a rough surface fiber of 14 mm long obtained by using the OM, EDDM and BIDM are compared in Figure 3. Compressed image of the same fiber obtained using the OM is inserted in the figure. As explained in the experimental section, this image was prepared by compressing the consecutively aligned images of the fiber along the fiber axis. It can be seen that the data from EDDM matched quite well with the data from OM, meanwhile the data from BIDM showed smoother variation of fiber diameter because of its lower positional resolution. In order to conduct the quantitative analysis on the correlation of diameter data from the three different types of optical equipment, the diameter data from OM and BIDM were plotted against the data from EDDM of corresponding position in Figures 3-4 (a) and 3-4 (b), respectively. The correlation coefficient between the data from OM and EDDM showed fairly high value of 0.8894. In this case, it was found that the deviation of data from the two different sources is mainly caused by a slight mutual shift of the data of significant fluctuation along the fiber axis. On the other hand, the correlation coefficient between the data from BIDM and EDDM was only 0.3533 because of the smoothed data from BIDM.

3.3.2 Comparison of on-line and off-line measurements

As another typical example of off-line diameter measurement using the EDDM, diameter fluctuation of the rough surface fiber of 300 mm long prepared at the extrusion temperature of 245 ^{o}C is shown in Figure 3-5 (a). On the other hand, Figure 3-5 (b) shows the result of the moving average operation $\overline{D}(x)$ obtained using eq. (2) by setting the length of the smoothing filter, a, to be 33 mm. From the variation of absolute value of $D(x)-\overline{D}(x)$ along the fiber length as shown in Figure 3-5 (c), R_a value was evaluated.

Variation of R_a value with the change of the range of moving average, a, is summarized in Figure 3-6. The R_a value increased with the increase of the length of smoothing filter as expected and showed a tendency of saturation at around 10 mm. Consulting Figure 3-6, the length of smoothing filter of 33 mm was adopted arbitrarily for further analyses. Result of the similar analysis for the as-pun fiber obtained at the extrusion temperature of 255 ^{o}C is also shown in the figure. When the as-spun fiber has smooth surface, the R_a value remained at a low level irrespective of the length of the smoothing filter in this range.

As a typical example of on-line diameter measurement of the spin-line using the BIDM, the result obtained at a position of 1.0 m from the spinneret for the spinning with the extrusion temperature of 245 ^{o}C is shown in Figure 3-7 (a). It should be noted that even though positional resolution of the BIDM is low in comparison with the apparent characteristic size of the surface roughness observed under microscope as shown in Fig.1, diameter fluctuation of short range was observed along with that of long range. When extrusion temperature was increased to 255 ^{o}C, only the long range fluctuation was observed. Therefore, it was conjectured that the long range fluctuation is attributable to the instability of the spinning process whereas the short range fluctuation is related with the development of surface roughness.

Result of the moving average operation for the data shown in Figure 3-7 (a) with the smoothing filter of 0.1 s and the absolute value of $D(x)-\overline{D}(x)$ are shown in Figures 3-7 (b) and (c), respectively. Even though the spin-line diameter showed long- and short-range fluctuations, the variation of short-range could be extracted successfully by using the smoothing filter of 0.1 s.

Melt spinning of PA6/PET was conducted under various spinning conditions, and the R_a values obtained through the on-line measurement using the BIDM and those for the as-spun fibers measured using the EDDM are compared in Figure 3-8. Fairly high positive correlation coefficient of 0.7573 was obtained between the R_a values from on-line and off-line measurements. This result suggests the possibility of analyzing the

surface roughness development behavior in the spin-line through the on-line measurement using the BIDM even though positional resolution of this apparatus is not high.

3.3.3 On-line measurement of spin-line diameter at various positions

On-line measurement of spin-line diameter was performed at various positions along the spin-line for the melt spinning of PA6/PET blend at the extrusion temperatures of 245 and 255 ^{o}C. Mean diameters analyzed by averaging the diameter data of 5 seconds obtained using the BIDM are plotted against the distance from spinneret in Figure 3-9. The spin-line diameter decreased with the increase of distance from the spinneret, and the diameter at 1.3m was still slightly higher than the diameter of as-spun fibers, which are shown as "off-line" diameters. Spin-line thinning delayed slightly when the extrusion temperature was higher. In this spinning condition, solidification of the spin-line is expected to occur when the spin-line temperature reaches the glass transition temperature of PA6. Delay in the cooling behavior caused by the higher extrusion temperature leads to the downward shift of the solidification point in the spin-line.

Time-course variations of spin-line diameter measured at various positions along the spin-line for the extrusion temperatures of 245 and 255 ^{o}C are shown in Figures 3-10 (a) and (b) respectively. Reduction of spin-line diameter with the increase of distance from the spinneret can be confirmed even though there was a certain level of long-range instability at both extrusion temperatures. On the other hand, as previously stated in the discussion for Fig.6, only in the case of the lower extrusion temperature of 245 ^{o}C, short-range diameter fluctuation was observed especially at positions far enough away from the spinneret. This short range fluctuation is considered to be originated from the development of surface roughness.

The abscissa in Figure 3-10 (a) and (b) can be converted from "Time" to "Length" using the local spin-line velocity, v. The equation of continuity as expressed in eq. (3)

can be applied for the estimation of V from the measured mean diameter.

$$W = \frac{\pi}{4} D^2 \rho V \quad \text{-------} (3)$$

where W is the through-put rate, D and ρ are the diameter and density of the spin-line. Considering the blend ratio of PA6/PET = 80/20 wt%, constant melt density of 1.019 g/cm^3 was assumed in the calculation [3, 4]. Then the horizontal axis can be converted through the relation: Length = Velocity x Time. This means that the positional resolution varies depending on the local spin-line velocity. Nevertheless, at the take-up velocity of 270 m/min and sampling rate of 1 kHz, corresponding positional resolution is 4.5 mm. The relations between diameter and length for the extrusion temperatures of 245 and 255 ^{o}C obtained after converting "Time" to "Length" are shown in Figure 3-11 (a) and (b). The diameter fluctuation with the amplitude of 10 – 20 μm was observed with a reasonably high positional resolution. It should be noted here that no characteristic period could be found through the application of Fourier transform analysis for the data shown in Figures 3-10 and 3-11.

Variations of the short-range fluctuation of spin-line diameter, Ra, and that standardized by the local mean diameter, R_a/D, are plotted against the distance from the spinneret in Figure 12. For the extrusion temperature of 245 ^{o}C, the roughness represented by the Ra value increased with the increase of distance from the spinning nozzle and almost saturated at around 0.7 m, whereas there was an additional increase of R_a/D value because of the continued decrease of the spin-line diameter. The R_a and R_a/D values for the extrusion temperature of 255 ^{o}C remained at low levels and only slight increases of both parameters with an increase in the distance from the spinneret were observed.

In the previous chapter, it was concluded that the conditions necessary for the development surface roughness are: (1) the minor component is a crystalline polymer; (2)

the major component can be either amorphous or crystalline polymer, but needs to be melt processable at a temperature lower than the melting temperature of the minor component; and (3) extrusion temperature is lower than the melting temperature of the minor component. It was also confirmed for the co-polyamide/PET blend fibers that the crystallization of the PET component proceeds in the spinning process only for the spinning with surface roughness development, and the PET component in the fiber maintains its high crystallizability even after its melting when the PET component was crystallized and surface roughness was developed in the spinning process. These results suggested the occurrence of the shear or elongational flow-induced crystallization of PET in the spinning head under its super-cooled state. Gradual development of the surface roughness in the spin-line along with its thinning confirmed in this research may indicate that the PET component exists in a state of low flow-ability at the moment of extrusion from the spinneret, and the protrusion of such solid-like part from the fiber surface proceeds during the thinning of the major component, PA6, which maintains its high flow-ability.

3.4 Conclusions

Three kinds of optical equipment were applied for the quantitative evaluation of surface roughness of PA6/PET blend fibers with and without roughness. In this research, OM, SEM and EDDM measurements were applied for off-line measurements, on the other hand, BIDM measurement was applied for on-line measurement. Optimum calculation method of R_a value which stands for the variation of roughness took by BIDM and EDDM measurements was investigated. There was a fairly high correlation between the R_a values obtained from the off-line measurement of as-spun fibers using the EDDM and those from the on-line measurement of the spin-line using the BIDM. Utilizing such correlation, it was revealed that the roughness develops gradually with the increase of distance from the spinneret.

Reference

[1] Shirakashi Y, Asakura O, Ito S, et al. Development of polyamide 6 based blend fibers with surface roughness for artificial hair. Seikei-Kakou 2011; 23: 358-364.

[2] Xu X, Shirakashi Y, Ishibashi J, et al. Mechanism of surface roughness development in melt spinning of blend fibers for artificial hair, Text Res J 2012; 82(13), 1382-1389.

[3] Shimizu J, Okui N and Kikutani T. In: Ziabicki A and Kawai H (eds) High-speed fiber spinning. New York: Wiley & Sons, 1985, pp.173-206.

[4] Brandrup J, Immergut EH (eds) Polymer Handbook. 2nd ed. New York: Wiley & Sons, 1989.

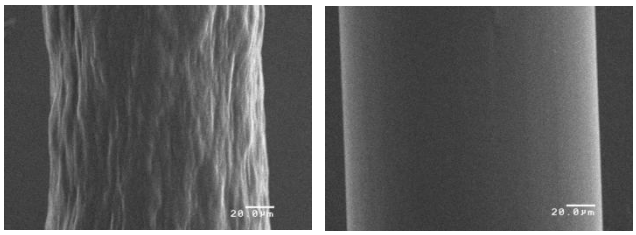

(a) **(b)**

Figure 3-1. Scanning electron micrographs of PA6/PET blend fibers prepared at the extrusion temperatures of (a) 245 ^{o}C and (b) 255 ^{o}C. Take-up velocity, through-put rate and nozzle diameter are 270 m/min, 5.8 g/min and 0.5 mm, respectively.

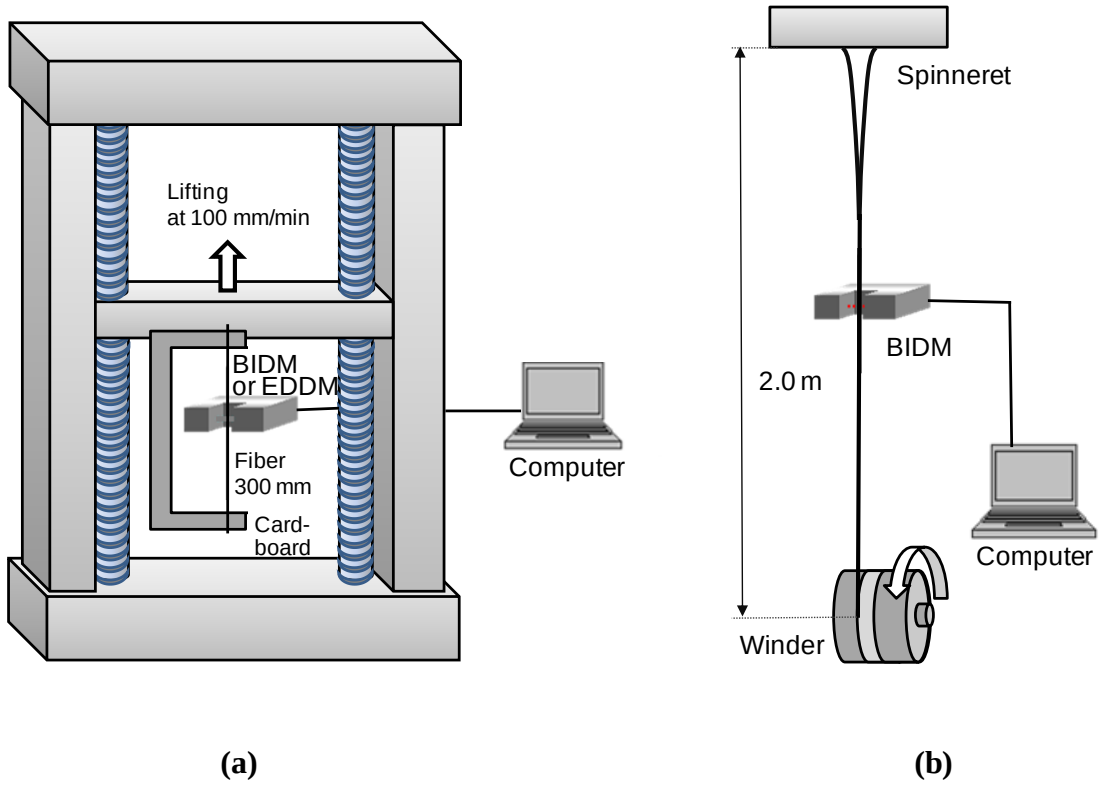

Figure 3-2. Schematic diagram of (a) off-line and (b) on-line measurement systems for fiber diameter variation.

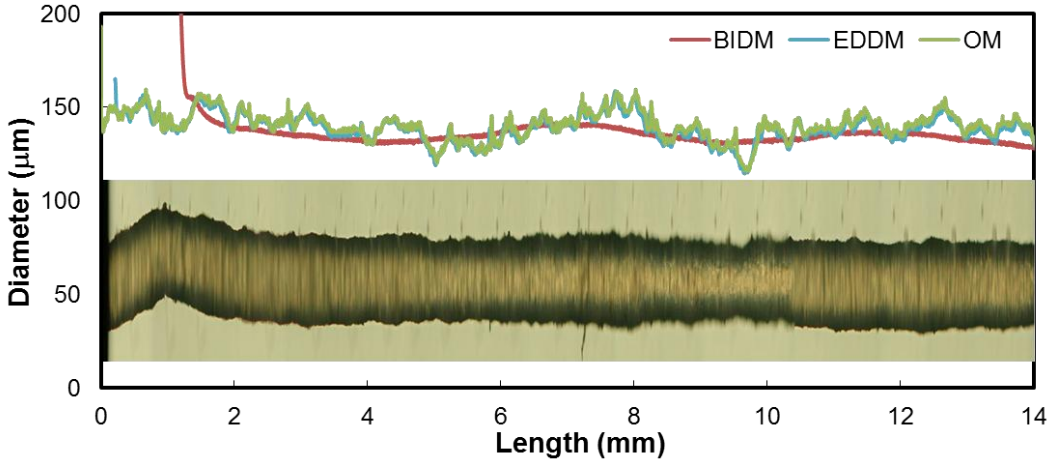

Figure 3-3. Comparison of the diameter profiles of as-spun rough-surface PA6/PET fiber measured using three types of optical apparatuses, optical microscope (OM), edge detection type diameter monitor (EDDM) and back-illumination type diameter monitor (BIDM). Compressed image of the consecutively aligned photographs of fiber sample taken by OM is also shown.

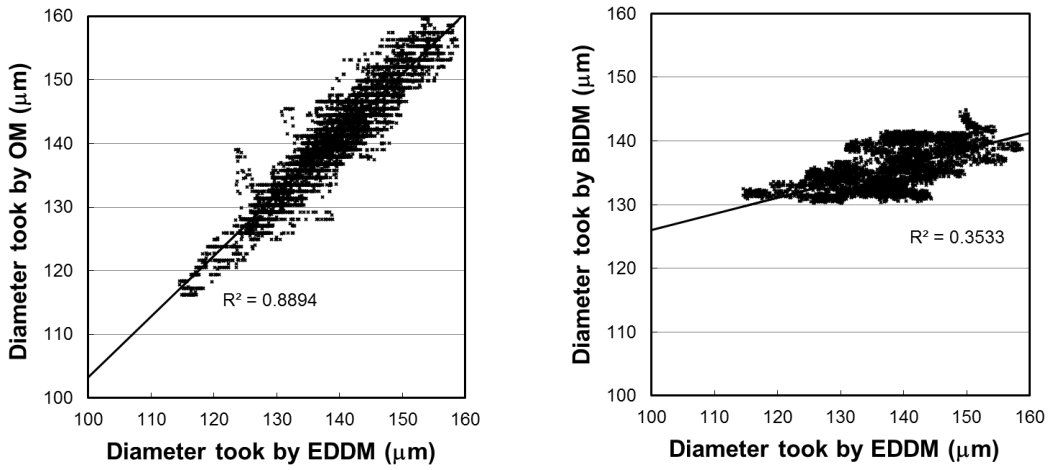

(a) **(b)**

Figure 3-4. Relation between the fiber diameter variations obtained using three different types of optical equipment. The analyzed region is from 1.3 to 14 mm along the fiber axis shown in Figure 3-3. (a) Comparison of fiber diameters took by EDDM and OM. (b) Comparison of fiber diameters took by EDDM and BIDM.

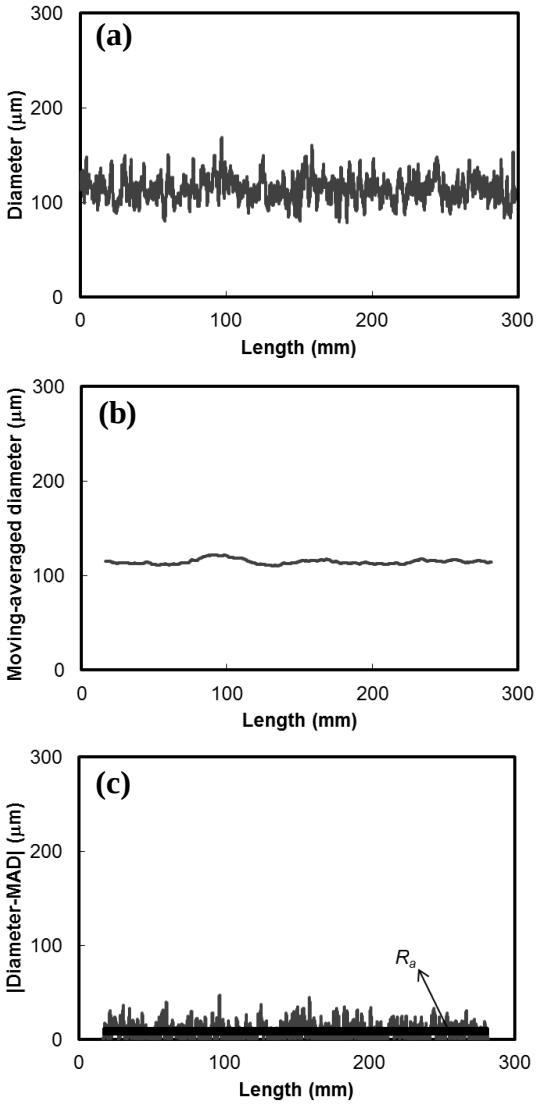

Figure 3-5. Analysis of diameter variation for the as-spun rough-surface PA6/PET fiber prepared at take-up velocity 270 m/min, through-put rate 5.8 g/min, nozzle diameter 0.5 mm and extrusion temperature 245 ^{o}C. (a): Diameter variation along the fiber axis measured using EDDM. (b): Result of moving-average operation for data (a) with the smoothing filter of 33 mm. (c): Result of the subtraction of data (b) from data (a). MAD is moving-averaged diameter. Mean value R_a is indicated as a straight line.

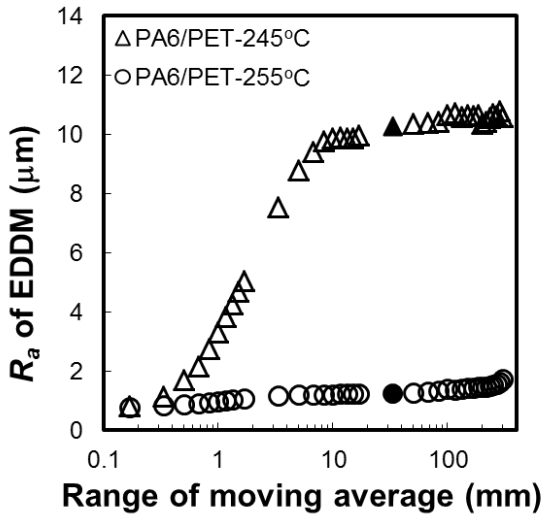

Figure 3-6. Effect of the range of moving average on the R_a values for the PA6/PET fibers prepared at the extrusion temperatures of 245 and 255 °C. The fibers are same as those shown in Figure 3-1. Take-up velocity and through-put rate are 270 m/min and 5.8 g/min, respectively. Moving average of 33 mm which is marked with closed symbols is applied for analysis of *R*a value from off-line diameter data measured by EDDM in this study.

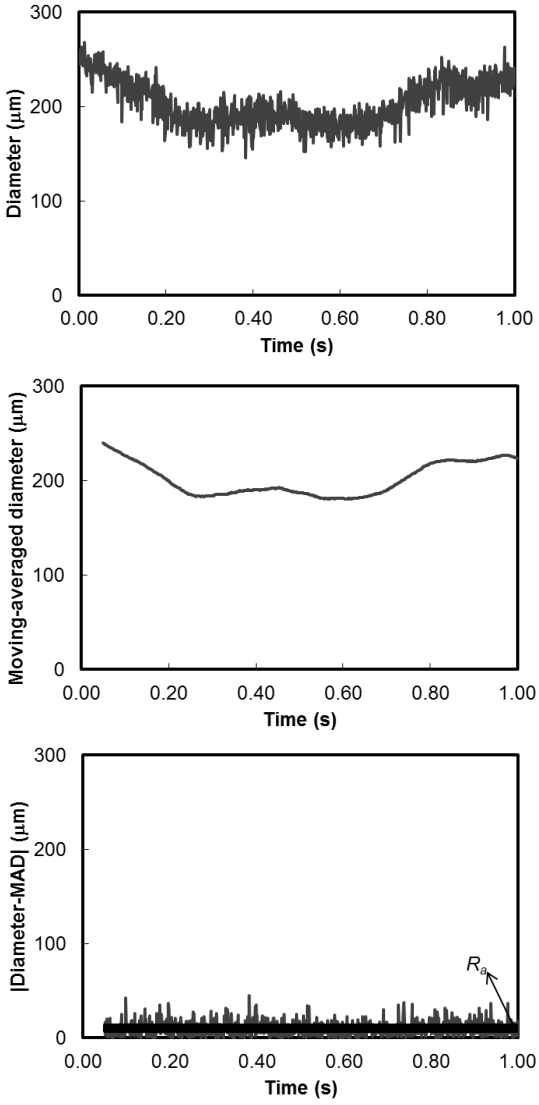

Figure 3-7. Analysis of diameter variation from on-line measurement of the spin-line for PA6/PET spinning at take-up velocity 270 m/min, through-put rate 5.8 g/min, nozzle diameter 0.5 mm and extrusion temperature 245 ^{o}C. (a): Time-course diameter variation measured at 1.0 m from the spinneret using BIDM. (b): Result of moving-average operation for data (a) with the smoothing filter of 0.1 s. (c): Result of the subtraction of data (b) from data (a). MAD is moving-averaged diameter. Mean value R_a is indicated as a straight line.

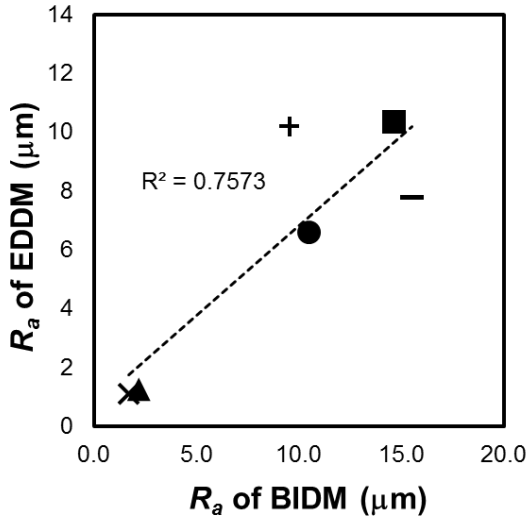

Figure 3-8. Correlation between R_a values from off-line measurement for as-spun PA6/PET fibers using EDDM and those from on-line measurement of the spin-line using BIDM. Spinning conditions (take-up velocity, through-put rate and extrusion temperature) for various degrees of surface roughness are: ■ 124 m/min-5.8 g/min-240 °C; − 124 m/min-3.0 g/min-240 °C; ● 124 m/min-5.8 g/min-245 °C; + 270 m/min-5.8 g/min-245 °C; ▲ 270 m/min-5.8 g/min-255 °C; × 270 m/min-3.0 g/min-255 °C. Correlation coefficient is also shown in the figure.

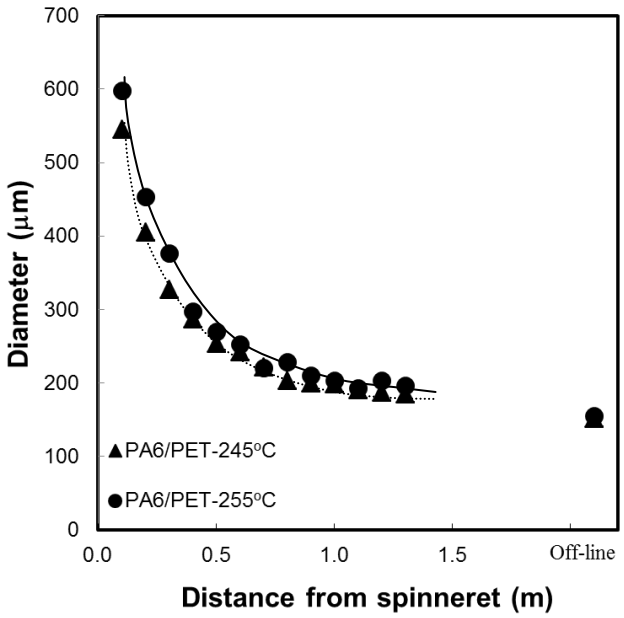

Figure 3-9. Variations of spin-line diameter with the increase of distance from spinneret for PA6/PET spinning at the extrusion temperatures of 245 and 255 ^{o}C. Take-up velocity, through-put rate, nozzle diameter are 0.27 m/min, 5.8 g/min and 0.5 mm, respectively. Measurement was performed using BIDM for 5 s at each position and the mean values are plotted in the figure. Results of off-line measurement for the as-spun fibers are also indicated.

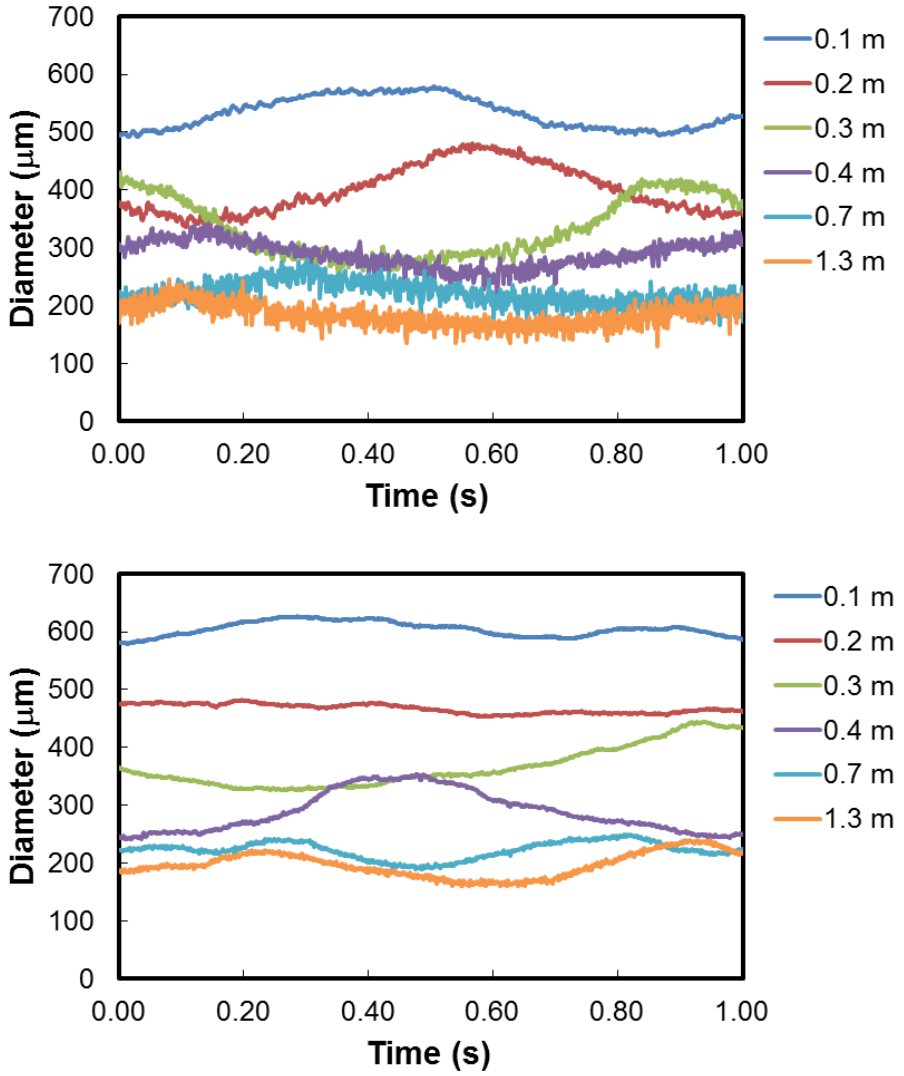

Figure 3-10. Time-course diameter variations measured using BIDM at various positions along the PA6/PET spin-line for the extrusion temperatures of (a) 245 ^{o}C and (b) 255 ^{o}C. Take-up velocity, through-put rate and nozzle diameter are 270 m/min, 5.8 g/min and 0.5 mm, respectively.

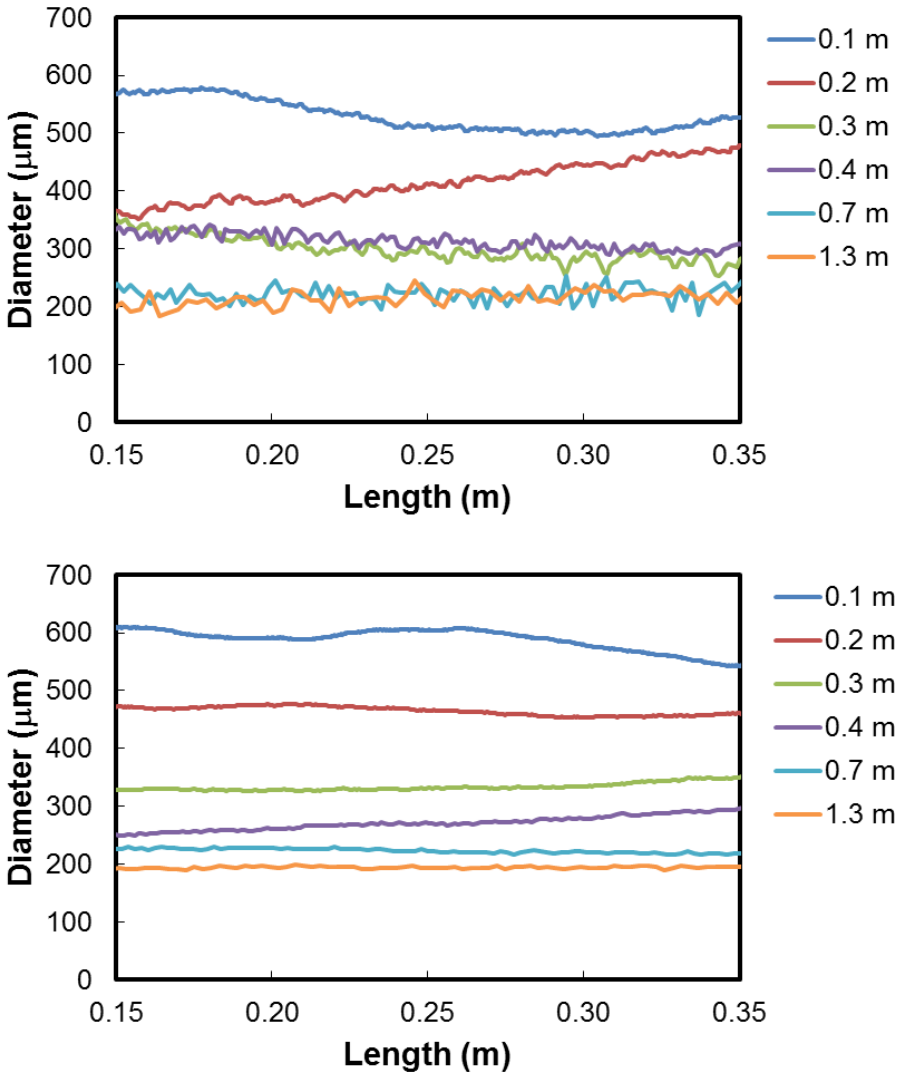

Figure 3-11. Diameter variations of spin-line along fiber-length prepared from the data shown in Fig.10 by converting the abscissa from "Time" to "Length" using local spin-line velocity estimated from the mean diameter. Extrusion temperatures are (a) 245 ^{o}C and (b) 255 ^{o}C. Take-up velocity, through-put rate and nozzle diameter are 270 m/min, 5.8 g/min and 0.5 mm, respectively.

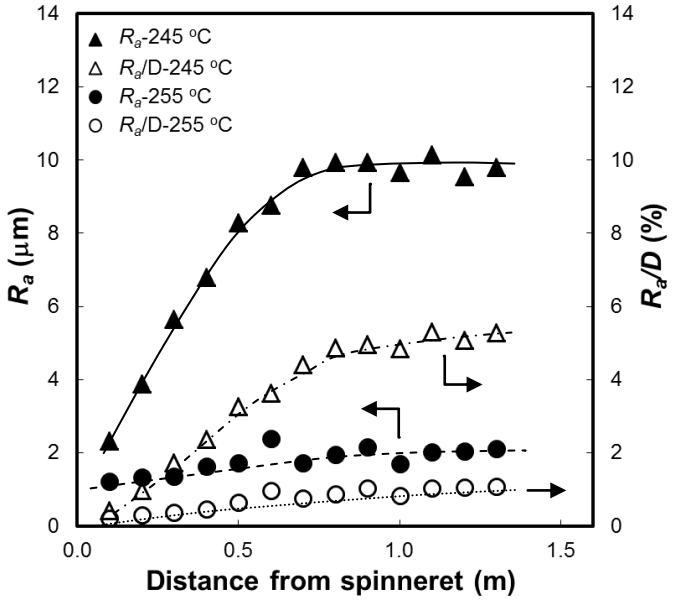

Figure 3-12. Variations of R_a and R_a/D values along the spin-line for PA6/PET spinning at extrusion temperatures of 245 and 255 °C. Take-up velocity and through-put rate are 0.27 m/min and 5.8 g/min, respectively. The R_a and R_a/D values are obtained by analyzing the data shown in Figure 5-14.

Chapter 4

Influence of Various Spinning Conditions on Surface Roughness Development in Melt spinning of PA6/PET Blend Fibers for Artificial Hair

4.1 Introduction

4.2 Experimental

4.2.1 Materials and Melt Spinning Conditions

4.2.2 Scanning Electron Microscope

4.2.3 Edge Detection type Diameter Monitor

4.2.4 Wide Angle X-ray Diffraction

4.2.5 Differential Scanning Calorimetry

4.2.6 High Speed Camera

4.3 Results and Discussion

4.3.1 Effect of Extrusion Temperature

4.3.2 Effect of Nozzle Diameter

4.3.3 Effect of Through-put Rate

4.3.4 Effect of Take-up Velocity

4.3.5 Effect of Water Bath

4.3.6 Effect of the Intrinsic Viscosity of PET Component

4.4 Conclusions

Reference

Chapter 4

Influence of Various Spinning Conditions on Surface Roughness Development in Melt spinning of PA6/PET Blend Fibers for Artificial Hair

4.1 Introduction

In chapter 2, it has been reported that fibers for artificial hair with developed surface roughness can be produced in melt spinning of polyamide 6 (PA6)/ poly(ethylene terephthalate) (PET) under certain spinning conditions [1] [2]. In order to clarify the surface roughness development behavior, effect of various spinning conditions on the roughness of fibers was investigated in this chapter. The spinning conditions investigated included the extrusion temperature, nozzle diameter, through-put rate and take-up velocity. Effects of water bath applied in the spinning process and the intrinsic viscosity of PET component were also investigated. Roughness of as-spun fibers was quantitatively analyzed by the edge-detection type diameter monitor (EDDM). For some samples, the crystallization behavior was also investigated using wide angle X-ray diffraction (WAXD) and differential scanning calorimetry (DSC).

4.2 Experimental

4.2.1 Materials and Melt Spinning Conditions

The materials we applied in this chapter were PA6 (NOVAMID 1020, DSM Japan Engineering Plastics), PET1 (PETMAX RE530A, Toyobo Co., Ltd.) with Intrinsic Viscosity ≈ 0.624, PET2 (SA-1206, Yamaso Co., Ltd) with Intrinsic Viscosity ≈ 1.07. Dry-blended polymer pellets of PA6 and PET1 (PET2) with mass ratio of 80:20 were melted and extruded using an extrusion system consisting of a co-rotating twin-screw extruder, a gear pump and a spinneret with a single-hole nozzle of 0.5, 1.0, 2.0 mm diameter, respectively. Take-up winder was placed at a position 2.0 m below the spinneret.

Through-put rate were set to 3.0 or 5.8 g/min and take-up velocities changed in the range of 0.27 ~ 4.0 km/min. Barrel temperatures C1 - C4, i.e. the zone temperatures from upstream to downstream in the extruder, were 160, 260, 235 and 235 ^{o}C. It should be noted that the highest temperature in the extruder was set to be higher than the melting temperatures of PA6 (220 ^{o}C), PET (257 ^{o}C) and PET2 (251 ^{o}C), whereas the extrusion temperature was adjusted in the region of the metering pump and the spinneret. More detailed spinning conditions for as-spun fibers discussed in this chapter are shown in Table 1. The lowest extrusion temperatures of fibers spun with nozzle diameter of 0.5, 1.0 and 2.0 were 235, 235 and 255 ^{o}C, respectively. The gear pump could be broken if the lower extrusion temperature was applied in each case. Water bath was applied for the spinning conditions of nozzle diameter 2.0 mm, extrusion temperature 255 ^{o}C, and take-up velocity 0.27 km/min. The distance between water bath and spinneret was 0.7 m.

4.2.2 Scanning Electron Microscope

Surfaces of as-spun fibers were analyzed using a scanning electron microscope (SM-200: TOPCON Co., Ltd) with magnification of 500x.

4.2.3 Edge Detection type Diameter Monitor

Edge detection type diameter monitor (EDDM) (LS-7010M: KEYENCE Co., Ltd.) was applied as off-line measurement. 300 mm length as-spun fiber sample was fixed to a cardboard frame was moved along the fiber axis with a speed of 100 mm/min to pass through the measurement area of EDDM. The positional resolution for the direction of fiber axis, sampling rate and effective measurement area are 30 μm, 50 Hz and 2 x 4 mm, respectively. Device resolutions of EDDM for the measurement of fiber diameter are 0.5 μm.

4.2.4 Wide Angle X-ray Diffraction

Crystalline structure in the as-spun fibers was analyzed through the wide-angle X-ray diffraction (WAXD) measurement. The two-dimensional WAXD intensity distribution

measurement for the fiber bundles was performed using a nickel-filtered CuKα radiation source generated at 60 kV-45 mA and a Mercury CCD X-ray detector (Rigaku Co., Ltd.) at a camera length of 35 mm. For each measurement, exposure time of 50 s was repeated for 5 times.

4.2.5 Differential Scanning Calorimetry

Thermal analysis of the as-spun blend fibers was conducted through the differential scanning calorimetry (DSC, TA Instruments.) at the heating and cooling rates of 10 K/min and 40 K/min, respectively. In the DSC measurement process, PA6/PET blend fibers were cut to be powder-like pieces, with the weight of 5 mg. Powder like fibers were heated up to from 20 ^{o}C to 280 ^{o}C with heating rate of 10 ^{o}C/min, then cooled to 20 ^{o}C with cooling rate of 40 ^{o}C, immediately.

4.2.6 High Speed Camera

Images of fibers just extruded from the spinneret were taken by high speed camera (HSC, Vision Research, Inc.) with lens supplied by Nikon, Co., Ltd.

4.3 Results and Discussion

4.3.1 Effect of Extrusion Temperature

In the previous chapters, it has been clarified that rough surface synthetic fiber can be obtained by the melt spinning of PA6 blended with PET1 with the mass ratio of 80/20 at certain spinning temperatures. The SEM photographs of PA6/PET1 blend fibers spun with different extrusion temperatures are shown in Figure 4-1. Obviously, it can be seen that, with the same nozzle diameter, roughness decreased with increasing extrusion temperature. The relationship between roughness and extrusion temperature was very clear. The most remarkable roughness appeared with the nozzle diameter of 1.0 mm. It also have been explained the R_a value of as-spun fibers took by EDDM could evaluate the roughness on the surface of fiber. The R_a values of various as-spun fibers are shown in Figure 4-2.

As same as the SEM results, it can be found that with the same nozzle diameter, the roughness was enhanced by lowering the extrusion temperature, meanwhile, the maximum R_a values of fibers spun with nozzle diameter of 1.0 mm were higher than other fibers spun with nozzle diameter of 0.5 and 2.0 mm. It should be noticed that the extrusion temperature in this research means the setting temperature of the spinneret and gear pump. There can be a difference between extrusion temperature and polymer temperature in the nozzle.

4.3.2 Effect of spinneret diameter

From both SEM photographs and R_a values, it can be found that, even with the same extrusion temperature of 255 ^{o}C, roughness decreased with smaller nozzle diameter. That can be explained considering the viscous heating of polymer in the spinneret. The change of temperature of polymers in the spinneret was calculated by following formulas:

$$\frac{\pi R^4}{8}\frac{\Delta P}{\eta L} = \frac{W}{\rho} \qquad \text{.....(4.1)}$$

$$\Delta T = \frac{\Delta P}{\rho C_p} \qquad \text{.....(4.2)}$$

Where C_p is the heat capacity (1.54 J/K), ρ is the density (1160 kg/m^3), [7, 8], ΔP is the pressure, η is the shear viscosity of the blend polymer, R and L are the radius and length of the spinning nozzle. [3] [4] Assuming the viscosity η of 200 Pa·s, temperature increases ΔT was:

D (mm)	L (mm)	η (Pa·s)	ΔT (^{o}C)
2.0	5.0		0.14
1.0	3.0	200	1.34
0.5	1.0		7.17

The temperature of polymer blends was increased significantly especially for smaller nozzle diameter. With spinneret diameter of 1.0 mm, the increase of temperature of polymer blends was 1.34 ^{o}C, meanwhile the extrusion temperature can be lowered to 235 ^{o}C, as same as the lowest extrusion temperature of fibers spun with nozzle diameter of 0.5 mm. Considering the combination of the lowest extrusion temperature and temperature increase in the nozzle, the most enhanced roughness development for the nozzle diameter of 1.0 mm could be regarded as reasonable.

In the melt spinning process, a significant Barus effect was also observed as shown Figure 4-3. From the HSC photographs, it can be seen that the Barus effect was more enhanced with higher extrusion temperature where the surface of fiber was smooth. The same phenomenon can be obtained with other nozzle diameters of 0.5 and 2.0 mm, however, the relationship between Barus effect and roughness development cannot be clarified.

4.3.3 Effect of through-put rate

Through-put rates of 3.0 and 5.8 g/min were applied. From Figure 4-4, it can be seen that the R_a values of fibers spun with through-put rate of 5.8 g/min was slightly higher. However, the R_a/D values of fibers spun with the higher through-put rate of 5.8 g/min was lower than the fibers spun with the lower through-put rate of 3.0 g/min because of larger fiber diameters. The difference in the degree of surface roughness brought about by the through-put rate difference was not very obvious.

4.3.4 Effect of take-up velocity

Take-up velocities of fiber in melt spinning can influence the property of final products. Therefore, the effect of take-up velocity must be considered carefully. In this chapter, effect of take-up velocity will be discussed for the PA6/PET1 fibers spun with a nozzle diameter of 1.0 mm, extrusion temperature of 250 ^{o}C, take-up velocities of 0.27, 1.0, 2.0, 3.0 and 4.0 km/min. SEM photographs are shown in Figure 4-5. The fiber diameter decreased with the increase of take-up velocity because the through-put rate was kept

constant, whereas the change of roughness was difficult to be judged from the photographs. The R_a and R_a/D values of each fiber sample are shown in Figure 4-6. The R_a value decreased with the increase of take-up velocity, because of the enhanced extension of fiber along the spin-line. On the other hand, since the diameter of fiber decreased at higher take-up velocities, the R_a/D value increased with the take-up velocity.

4.3.5 Effect of Water Bath

PA6/PET1 Fibers spun with and without water bath are compared in Figure 4-7. It can be seen that the roughness was less developed when the water bath was used. The distance between spinneret and water bath was 0.7 m. Effect of the water bath on the spinning behavior can be considered as follows. Firstly, the thing behavior can be altered by the introduction of water bath. Without water bath, molten polymer blends was cooled and solidified slowly along the spin-line. On the other hand, when the water bath was applied, the spin-line can be cooled and solidified abruptly around the position of the water surface. Secondly, according to the wide angle X-ray diffraction (WAXD) patterns and intensity distribution curves for PA6/PET1 blend fibers melt spun with and without water bath shown in Figures 4-8 and 4-9, it can be found that for the fiber spun with water bath, the crystalline reflections of α-form (200) and (002+202) planes of crystals of PA6 component at the diffraction angles of 20.5 ^{o} and 23 ^{o}, respectively [5-9] can be observed. Since the glass transition point of PA6 decreased with the effect of water, the formation of α -form crystal of PA6 component was enhanced [10].

4.3.6 Effect of the Intrinsic Viscosity of PET Component

SEM photographs of PA6/PET1 and PA6/PET2 fibers are shown in Figure 4-10. At the same extrusion temperature, roughness development was suppressed if fibers were spun using the PET component of higher intrinsic viscosity. This phenomenon can also be explained by formulas 4.1 and 4.2. Higher viscosity could cause the increasing of temperature of polymer blends in the spinning nozzle, meanwhile the roughness decreased with the increase of temperature of polymer blends. It also has been found that

for the fibers with rough surface, crystallization of PET component was enhanced obviously [1]. In fact, with the extrusion temperature close to the melting temperature of PET, the crystallization of PET cannot proceed because of its quite slow crystallization rate. Therefore, in our research, the crystallization of PET component was considered to be achieved by the effect of flow in the melt spinning equipment. The stress accompanied with the polymer flow varies quite sensitively with the variation of the intrinsic viscosity, i.e. with the variation of molecular weight [11]. According to that theory, the use of high intrinsic viscosity PET should enhance the effect of flow and bring more remarkable roughness. However, from the SEM photographs, it was revealed that the roughness was decreased. This phenomenon suggested that the effect of polymer temperature increase was more effective in this case.

4.4 Conclusions

In this chapter, effects of several processing parameters in melt spinning process on the development of surface roughness were investigated. Surface roughness can be enhanced when extrusion temperature was lowered. Smaller nozzle diameter could lead to the increase of the true temperature of polymer blends in the spinning nozzle. Accordingly, the fibers produced using a nozzle of larger diameter showed higher degree of surface roughness at the same extrusion temperature. On the other hand, because of the combination of spinnability and possible extrusion temperature, the most developed roughness appeared with the nozzle diameter of 1.0 mm. The larger through-put rate and lower take-up velocity also lead to the increase in the R_a values of PA6/PET blend fibers, while the R_a/D values increased at the lower through put rate and higher take-up velocity where thinner fibers were produced. Lastly, incorporation of the water bath in the spin-line and the use of PET with higher intrinsic viscosity were found to cause the decrease of surface roughness.

Reference

[1] Xu X, Shirakashi Y, Ishibashi J, et al. Mechanism of surface roughness development in melt spinning of blend fibers for artificial hair. Text Res J; 82(13), 1382-1389, (2012).

[2] Shirakashi Y, Asakura O, Ito S, et al. Development of polyamide 6 based blend fibers with surface roughness for artificial hair. Seikei-Kakou 2011; 23: 358-364.

[3] Shimizu J, Okui N and Kikutani T. In: Ziabicki A and Kawai H (eds) High-speed fiber spinning. New York: Wiley & Sons, pp.173-206, (1985).

[4] Brandrup J, Immergut EH (eds) Polymer Handbook. 2nd ed. New York: Wiley & Sons, (1989).

[5] V. Malta, G. Cojazzi, A. Fichera, et al. A re-examination of the crystal structure and molecular packing of α-nylon 6. European Polymer J; Vol. 15. pp. 765-770, (1979).

[6] Brill R. Z Phys Chem B;53:61 – 74, (1943).

[7] Holmes DR, Bunn CW, Smith DJ. J Polym Sci;17:159 – 77 (1955).

[8] Kinoshita Y. Makromol Chem;33:1 – 20, (1959).

[9] Mingjun Yuan, Lih-Sheng TurngCorresponding, Polymer; Volume 46, Issue 18, 23, Pages 7273–7292, (2005)

[10] Cornelius T. Moynihan, Allan J. Easteal , James Wilder , Joseph Tucker. Dependence of the glass transition temperature on heating and cooling rate. J. Phys. Chem; 78 (26), pp 2673–2677, (1974).

[11] H. Münstedt, Dependence of the Elongational Behavior of Polystyrene Melts on Molecular Weight and Molecular Weight Distribution. J. Rheol. 24, 847 (1980).

Table 1. Conditions for melt spinning of blend fibers.

Polymers (80/20 wt%)	**Nozzle diameter（mm）**	**Barrel temperatures (°C)** C1 C2 C3 C4	**Extrusion Temperature (°C)**	**Take-up velocity (km/min)**	**Through-put rate (g/min)**
PA6/PET1	2.0	160 260 235 235	250	×	5.8
			255~265	0.27~4.0	
	1.0		235~255		
			260~265	×	
	0.5		235~255	0.27	5.8, 3.0
			260~265	×	
PA6/PET2	2.0		250~260	0.27	5.8

×: Fiber cannot be collected by take-up roller.

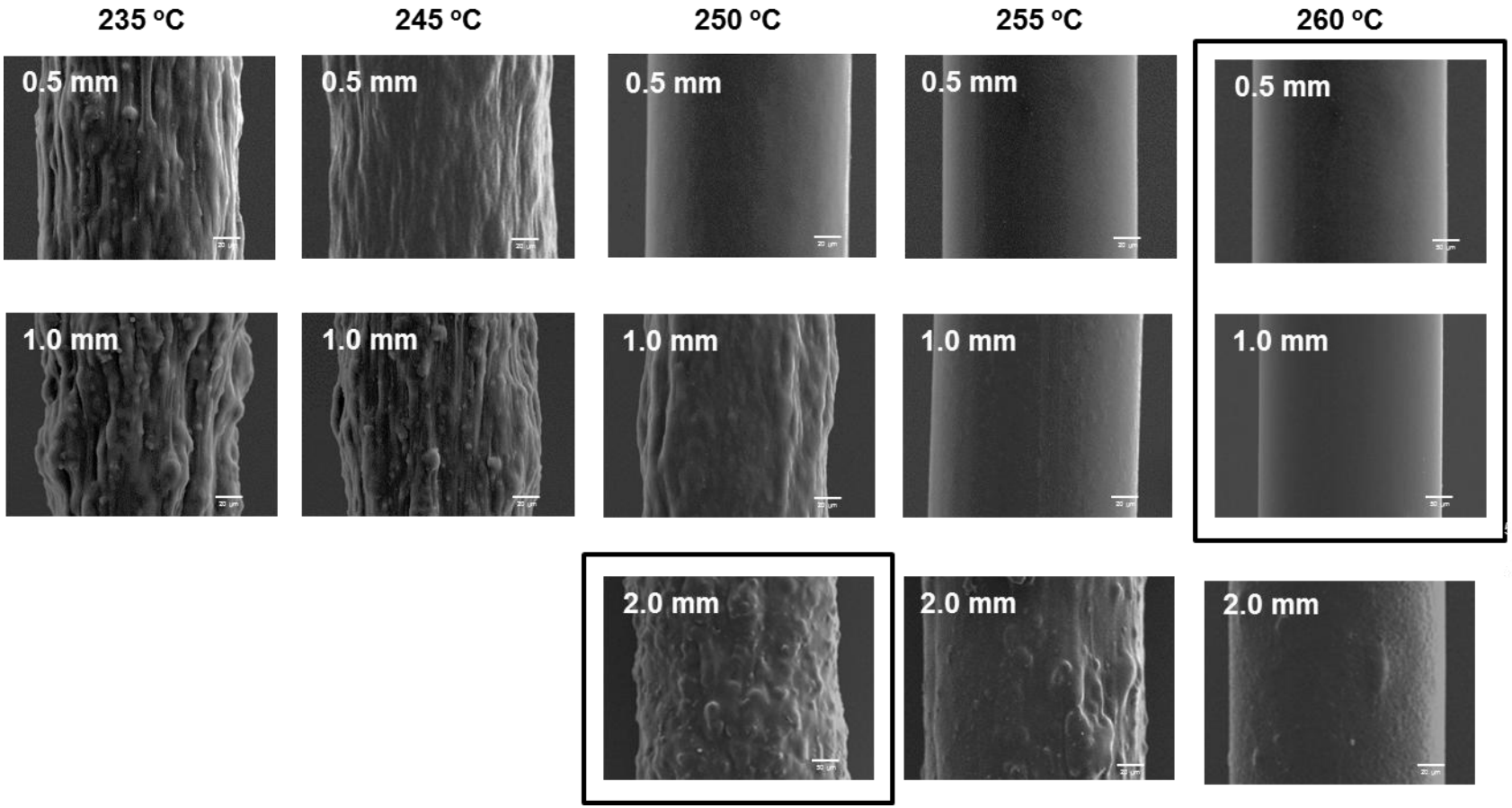

Figure 4-1. Scanning electron microscope (SEM) photographs of PA6/PET1 blend fibers melt spun with different nozzle diameters of 0.5, 1.0 and 2.0 mm, different extrusion temperatures from 235 to 260 ^{o}, with a through-put rate of 5.8 g/min and take-up velocity of 0.27 m/min. Fibers in the black frame cannot be taken by roller.

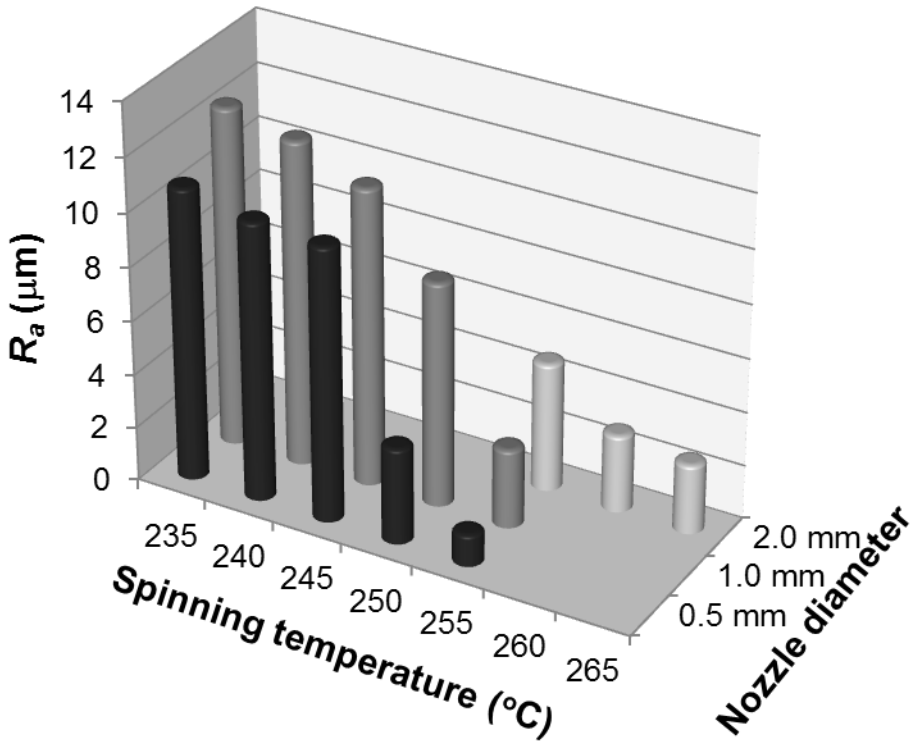

Figure 4-2. R_a values of PA6/PET1 blend fibers melt spun with different nozzle diameters of 0.5, 1.0 and 2.0 mm, different extrusion temperatures from 235 to 265 ^{o}C, with a through-put rate of 5.8 g/min and take-up velocity of 0.27 m/min.

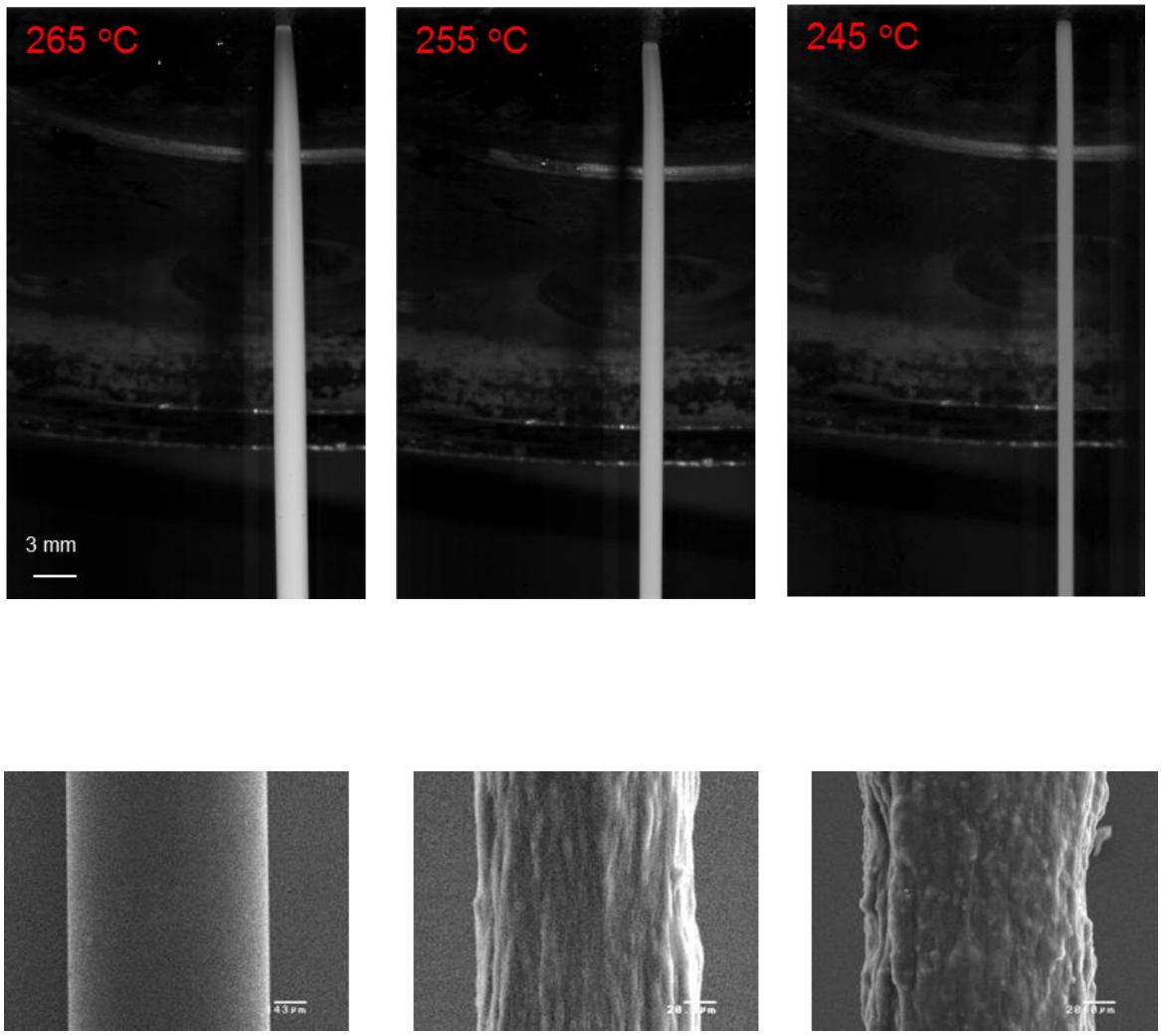

Figure 4-3. HSC photographs of fibers just extruded from the spinneret and SEM photographs of au-spun PA6/PET1 blend fibers spun with different extrusion temperatures of 245, 255 and 265 ^{o}C, with a nozzle diameter of 1.0 mm, through-put rate of 5.8 g/min and take-up velocity of 0.27 m/min.

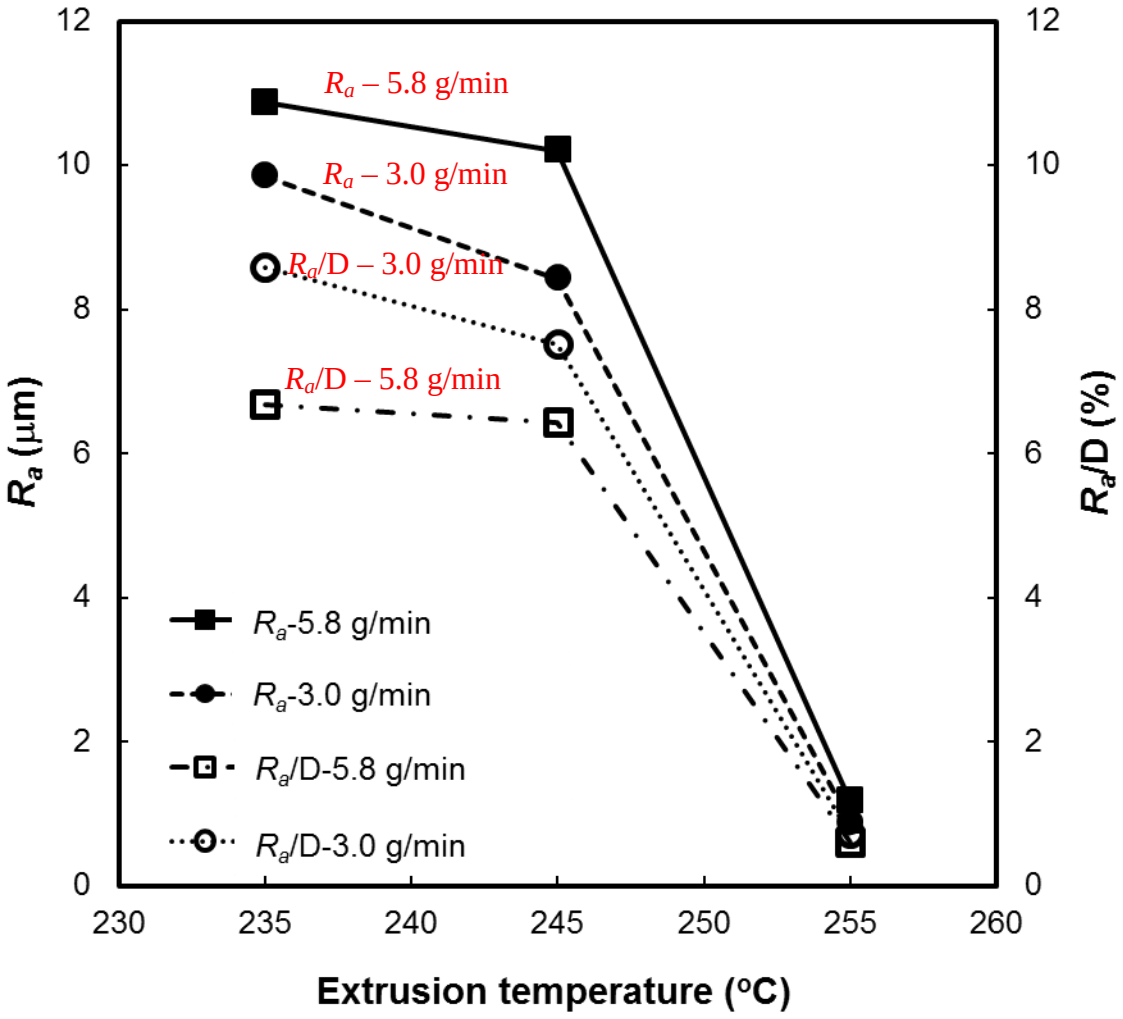

Figure 4-4. R_a and R_a/D values of PA6/PET1 blend fibers melt spun with different through-put rates of 5.8 and 3.0 g/min, different extrusion temperatures of 235, 245 and 255 ^{o}C, with a nozzle diameter of 0.5 mm and take-up velocity of 0.27 m/min.

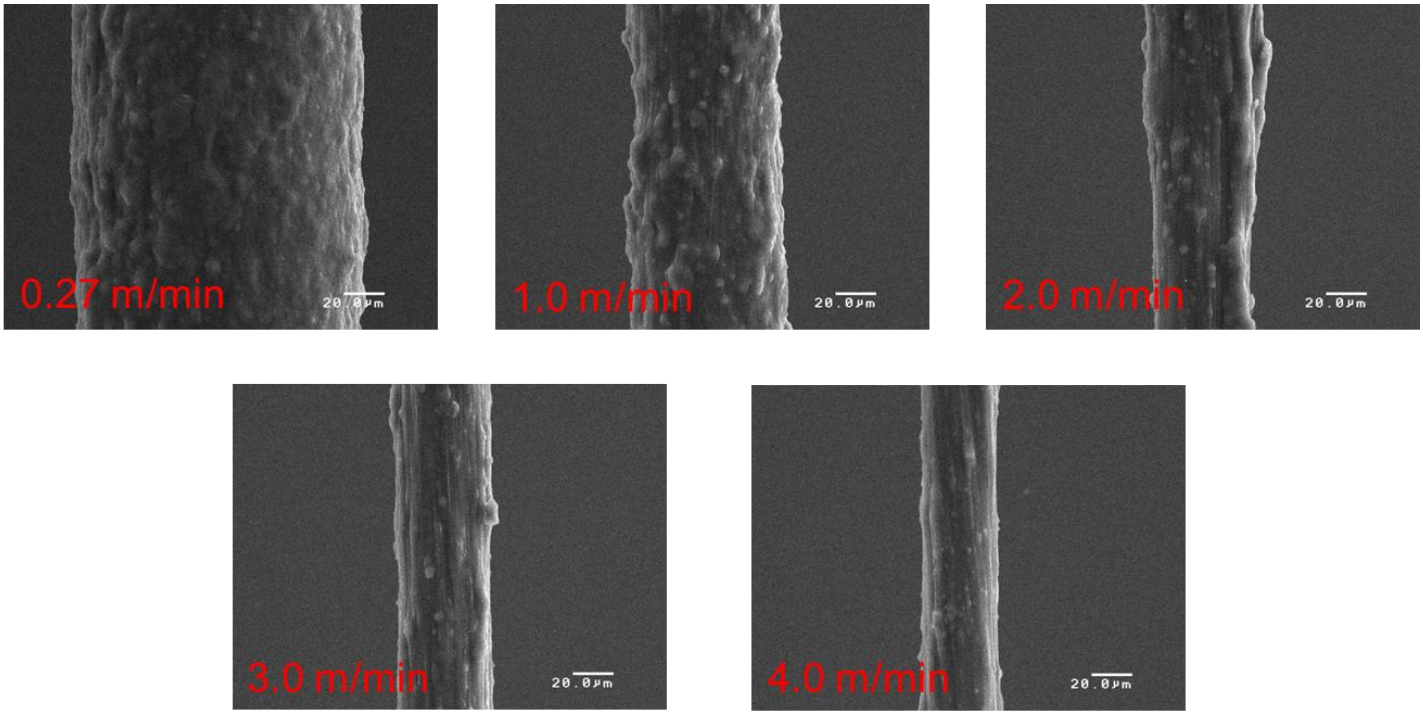

Figure 4-5. SEM photographs of PA6/PET1 blend fibers melt spun with different take-up velocities from 0.27 km/min to 4.0 km/min, with a nozzle diameter of 1.0 mm, through-put rate of 5.8 g/min, and extrusion temperature of 250 ^{o}C.

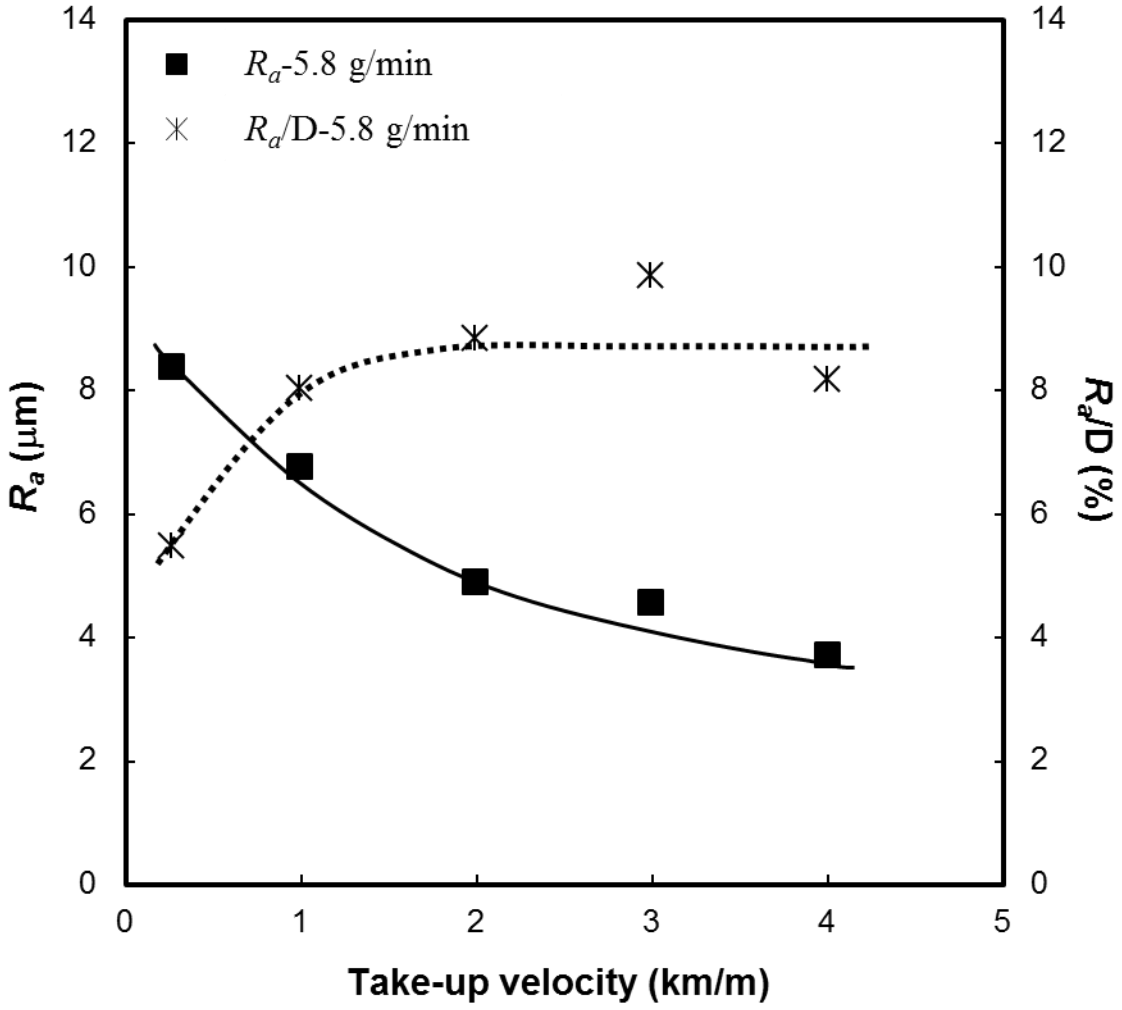

Figure 4-6. R_a and R_a/D values of PA6/PET1 blend fibers melt spun with different take-up velocities from 0.27 km/min to 4.0 km/min, with a nozzle diameter of 1.0 mm, through-put rate of 5.8 g/min, and extrusion temperature of 250 ^{o}C.

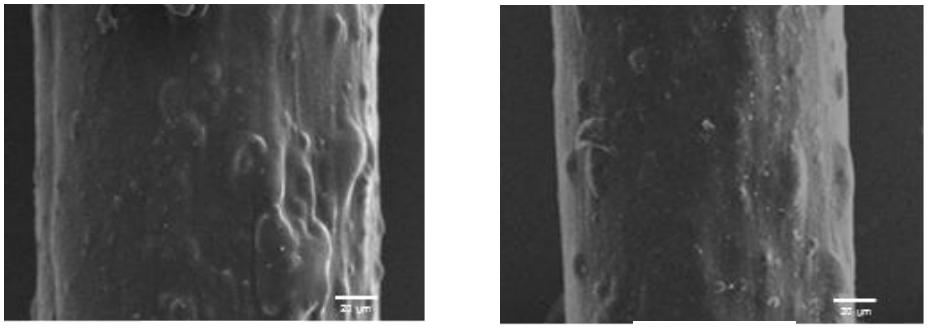

a. **b.**

Figure 4-7. SEM photographs of as-spun fibers melt spun with a take-up velocity of 0.27 km/min, extrusion temperature of 255 ^{o}C, nozzle diameter of 2.0 mm and through-put rate of 5.8 g/min. a. without water bath, b. with water bath.

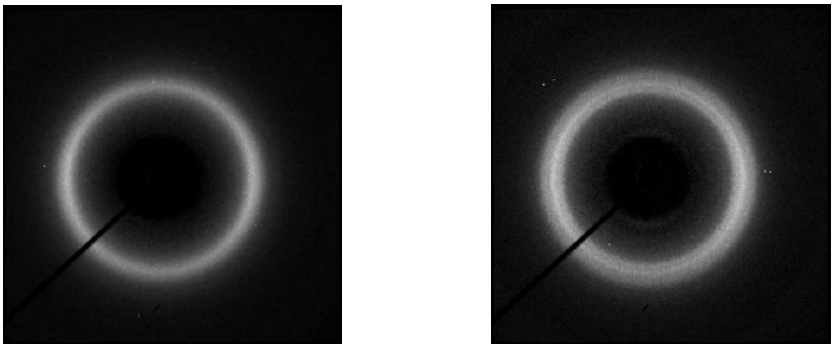

a. **b.**

Figure 4-8. Wide angle X-ray diffraction **(WAXD)** patterns of as spun PA6/PET1 blend fibers melt spun with a extrusion temperature of 255 ^{o}C, through-put rate of 5.8 g/min, nozzle diameter of 1.0 mm, take-up velocity 124 m/min. a. without water bath, b. with water bath.

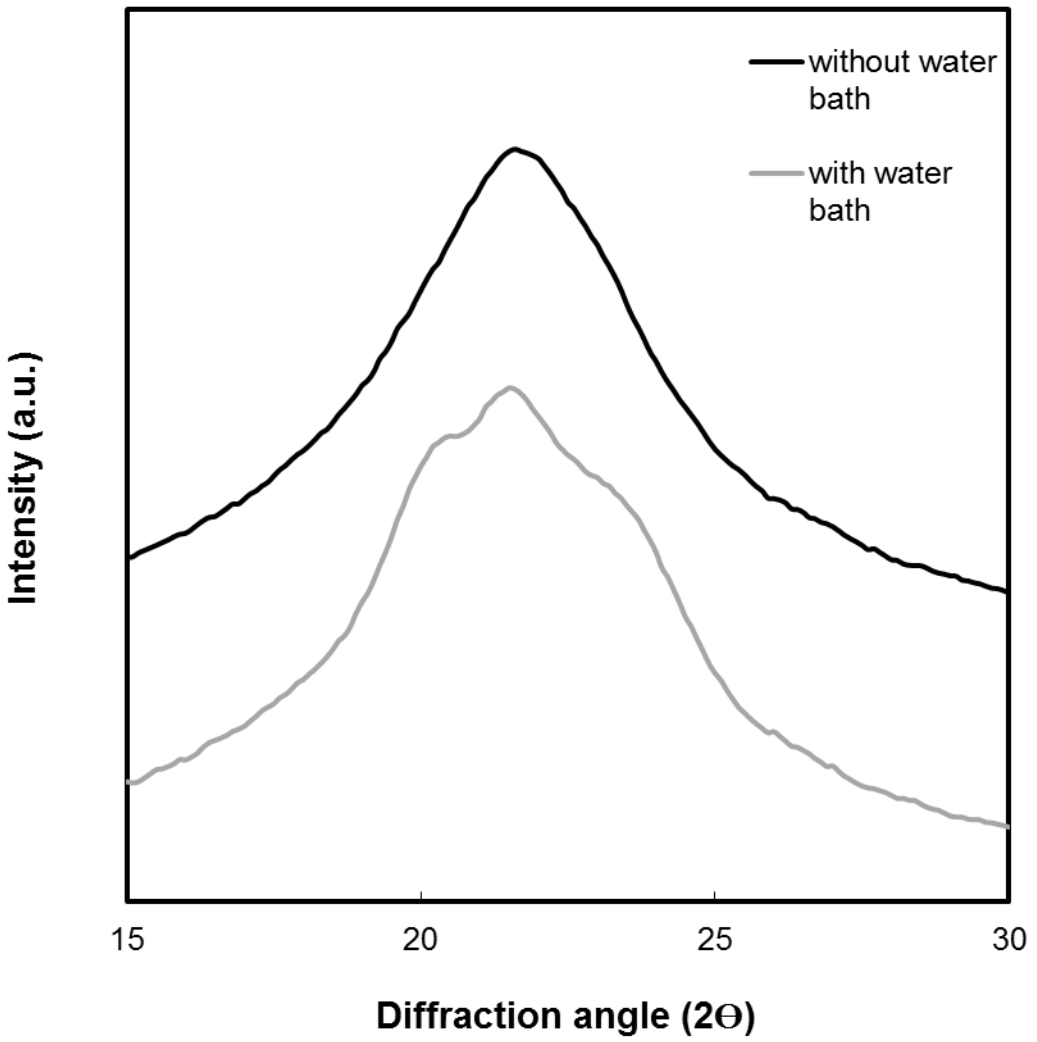

Figure 4-9. Wide angle X-ray diffraction (WAXD) intensity distribution curves for PA6/PET1 blend fibers melt spun with a extrusion temperature of 255 ^{o}C, through-put rate of 5.8 g/min, nozzle diameter of 1.0 mm, take-up velocity 124 m/min. a. without water bath, b. with water bath.

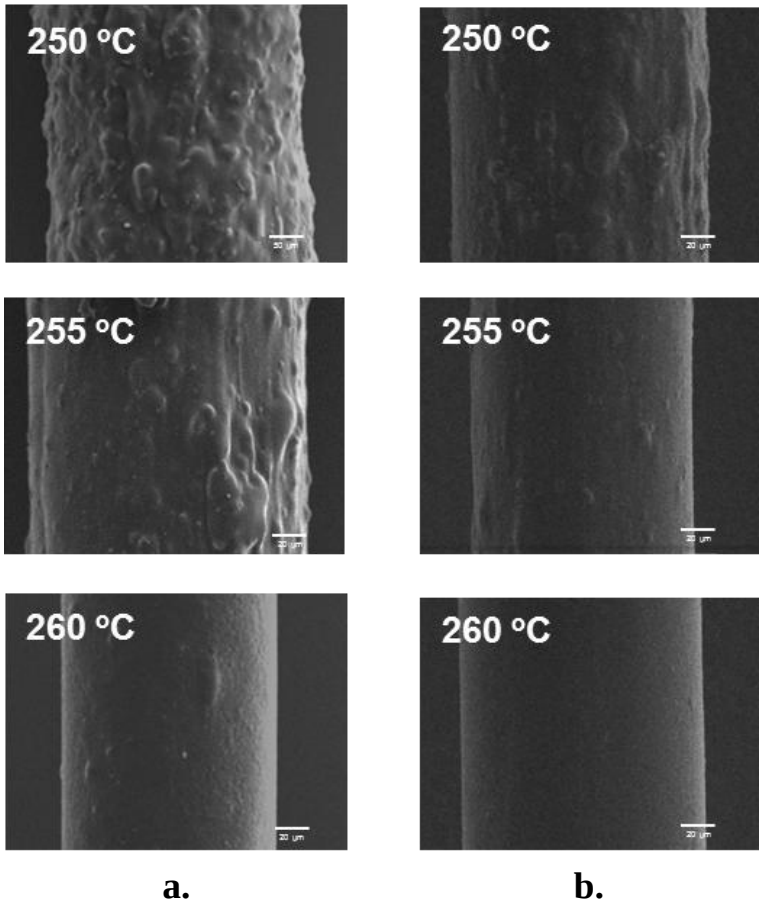

Figure 4-10. SEM photographs of PA6/PET1 and PA6/PET2 as-spun fibers melt spun with different extrusion temperatures of 250, 255 and 260 ^{o}C, respectively, with a nozzle diameter of 1.0 mm, through-put rate of 5.8 g/min and take-up velocity of 0.27 m/min. a. Intrinsic viscosity of PET1 ≈ 0.624. b. Intrinsic viscosity of PET2 ≈ 1.0

Chapter 5

Mechanism of Surface Roughness Development in Melt Spinning of PA6/PET Blend Fibers for Artificial Hair

5.1 Introduction

5.2 Experimental

5.2.1 Materials and Melt Spinning Conditions

5.2.2 Scanning Electron Microscope

5.2.3 Edge Detection type Diameter Monitor

5.2.4 Wide Angle X-ray Diffraction

5.2.5 Differential Scanning Calorimetry

5.2.6 Laser Microscope

5.2.7 Acid Treatment of Blend Fibers

5.3 Results and Discussion

5.3.1 Crystallization of PET Component of Rough and Smooth Surface PA6/PET Blend Fibers

5.3.2 Crystallization of PET Component of Rough and Smooth Surface co-PA/PET/PET Blend Fibers

5.3.3 Effect of Temperatures of Barrel, Adapter, etc.

5.3.4 Development of Roughness along the Spin-line

5.3.5 Differentiation of PET Component in PA6/PET Blend Fiber

5.4 Conclusions

Reference

Chapter 5

Mechanism of Surface Roughness Development in Melt Spinning of PA6/PET Blend Fibers for Artificial Hair

5.1 Introduction

In chapter 4, it has been clarified that although extrusion temperature is the most effective parameter for the development of surface roughness of PA6/PET fibers [1-2], various processing conditions in melt spinning process also showed a certain level of influence on the roughness development. In this chapter, the mechanism for the development of surface roughness will be discussed. The variation of roughness was measured by scanning electron microscopes (SEM1 and SEM2), back illumination type diameter monitor (BIDM), edge detection type diameter monitor (EDDM) and laser microscope (LM); the crystallization of as-spun fibers was confirmed by wide angle X-ray diffraction (WAXD) and differential scanning calorimetry (DSC). In addition, the formation of roughness was also studied from two sides: firstly, the effects of temperatures of twin-crew extruder and spinneret, secondly, the development process of roughness alone the spin-line. In order to explain the mechanism of formation of rough surface fiber we spun, the differentiation of PA6 and PET components of PA6/PET blend fiber was also carried out by alkali treatment of blend fibers and observing of axis and cross sections with SEM2.

5.2 Experimental

5.2.1 Materials and Melt Spinning Conditions

The materials we applied in this chapter were PA6 (NOVAMID 1020, DSM Japan Engineering Plastics), PET (PETMAX RE530A, Toyobo Co., Ltd.), amorphous co-polyamide (co-PA) (NOVAMID X21, DSM Japan Engineering Plastics). Firstly, dry-blended polymer pellets of PA6 and PET with mass ratio of 80:20 were melted and extruded using an extrusion system consisting of a co-rotating twin-screw extruder, a gear

pump and a spinneret with a single-hole nozzle of 0.5, 1.0, 2.0 mm diameter, separately. Take-up winder was placed at a position 2.0 m below the spinneret. Through-put rate were set to 5.8 g/min, and take-up velocities of 0.27 km/min. Secondly, dry-blended polymer pellets co-PA6 and PET with mass ratio of 80:20 were melted and extruded using the same extruder, a spinneret with a single-hole nozzle of 1.0 mm diameter and take-up velocity of 0.124 m/min, see table 1. The thirdly, as shown in table 2, dry-blended polymer pellets of PA6 and PET with mass ratio of 80:20 were melted and extruded with increased temperatures of the twin-crew extruder (C3~spinning head), adapter, etc. step by step. In this case, fiber samples (NO.1~NO.8) spun with a nozzle diameter of 1.0 mm, through-put rate of 5.8 g/min and take-up velocity of 50 m/min.

5.2.2 Scanning Electron Microscope

Surfaces of as-spun fibers were analyzed using scanning electron microscope (SEM1, SM-200: TOPCON Co., Ltd) with magnifications of 500 x and 1200x. Cross and axis sections were measured by another scanning electron microscope with energy dispersive X-ray detector-analysis (SEM2, 1450 VP, Zeiss Co., Ltd).

5.2.3 Edge Detection type Diameter Monitor

Edge detection type diameter monitor (EDDM) (LS-7010M: KEYENCE Co., Ltd.) was applied as off-line measurement. 300 mm length as-spun fiber sample was fixed to a cardboard frame was moved along the fiber axis with a speed of 100 mm/min to pass through the measurement area of EDDM. The positional resolution for the direction of fiber axis, sampling rate and effective measurement area are 30 μm, 50 Hz and 2 x 4 mm, respectively. Device resolutions of EDDM for the measurement of fiber diameter are 0.5 μm.

5.2.4 Wide Angle X-ray Diffraction

Amount of crystalline structure in the as-spun fibers was analyzed through the wide-angle X-ray diffraction (WAXD) measurement. The two-dimensional WAXD intensity

distribution measurement for the fiber bundles was performed using a nickel-filtered CuKα radiation source generated at 60 kV-45 mA and a Mercury CCD X-ray detector (Rigaku Co., Ltd.) at a camera length of 35 mm. For each measurement, exposure time of 50 s was repeated for 5 times.

5.2.5 Differential Scanning Calorimetry

Thermal analysis of the as-spun blend fibers was conducted through the differential scanning calorimetry (DSC, TA Instruments.) at the heating and cooling rates of 10 K/min and 40 K/min, respectively. In the DSC measurement process, PA6/PET blend fibers were cut to powder-like pieces. The powder like fibers of about 5 mg were heated from 20 to 300~310 ^{o}C with heating rate of 10 K/min, then cooled to 20 ^{o}C with cooling rate of 40 K/min. Before the starting of cooling, the temperature was kept constant for various holding times at the maximum temperature.

5.2.6 Laser Microscope

Fiber's surface was also observed by Laser Microscope (LM, OLS1100, OLYMPUS Co., Ltd.) Magnification was 50 x.

5.2.7 Alkali Treatment of Blend Fibers

PA6/PET blend fibers were treated by sodium hydroxide solution (20wt%) for 0.5 hour in the oil bath at temperature of 100 ^{o}C.

5.3 Results and Discussion

5.3.1 Crystallization of PET Component of Rough and Smooth Surface PA6/PET Blend Fibers

The analyses described in the previous chapters suggested that the crystallization of minor component is necessary for the development of surface roughness. From the view point of the crystallization kinetics of the minor component, however, crystallization of

the minor component PET was unlikely to take place within a short period in the extrusion and spinning processes even though the extrusion temperature was lowered to a temperature slightly below its melting point, where crystallization rate is estimated to be extremely low [3]. DSC thermograms and SEM photographs of PA6/PET blend fibers spun with different extrusion temperatures are shown in Figure 5-1. As it has been described in chapter 4, roughness was enhanced by lowering the extrusion temperature. The crystalline state of PET was also analyzed. In the measurement, the fiber samples were heated at a heating rate of 10 K/min up to 300 ^{o}C. In the heating process, although there was an influence of water adsorbed to PA6, clear cold crystallization peak of PET appeared at around 110 ^{o}C. More obvious cold crystallization peak appeared for fiber with smooth surface produced at high extrusion temperatures. Heat of cold crystallization of fibers spun with various spinning conditions are plotted against the polymer temperature at extrusion and R_a value as shown in Figure 5-2.

Temperature increases caused by viscous heating ΔT were calculated using Equations (4.1) and (4.2). By adding ΔT to the extrusion setting temperature (T), At different setting extrusion temperature, ΔT values for each nozzle diameter were different because viscosity of polymer changed with temperature. Viscosity η can be calculated by equation (5.1):

$$\eta = A\exp\left(\frac{E}{RT}\right) \qquad \text{.....(5.1)}$$

In that, E is activation energy, T is temperature, R is the molar gas constant and A is approximately a constant. At each nozzle diameter, with the lowest extrusion temperature, η was applied as 200 Pa·s. Actual polymer temperatures in the different spinning nozzles were estimated. With different setting temperatures, enhanced temperature ΔT values are shown in the following table:

Nozzle diameter: 0.5 mm			
T (^{o}C)	235	245	255
ΔT (^{o}C)	7.17	2.533	2.422
Nozzle diameter: 10 mm			
T (^{o}C)	235	245	255
ΔT (^{o}C)	1.34	0.473	0.452
Nozzle diameter: 2.0 mm			
T (^{o}C)	255	260	265
ΔT (^{o}C)	0.140	0.051	0.049

In Figure 4-1, it can be seen that fibers spun with 2.0 mm had relatively smooth surface. Meanwhile, according to Fig.6, heat of cold crystallization of those fibers kept as high values. That means the insufficient crystallization appeared for fibers with smooth surface. On the other hand, as fibers with roughness because of spun with low extrusion temperatures, the heat of cold crystallization can barely be observed. That means the more sufficient crystallization happened in melt spinning process of those fibers.

The 2-D intensity distribution obtained in the WAXD measurement was averaged along the azimuthal angle and plotted against the diffraction angle as shown in Figure 5-3. The obvious crystalline reflection at the diffraction angle of 26.1 degree, which was assigned to the (100) reflection from the triclinic crystal of PET [4], was observed obviously for the fibers prepared at the extrusion temperatures of 235 and 245 ^{o}C. This result clearly indicates that the crystallization of PET occurred in the melt spinning of PA6/PET blend when the surface roughness is developed because of low extrusion temperature. It has been introduced that the most obvious roughness appeared with the nozzle diameter of 1.0 mm. The integrated intensity values of various fibers were plotted against the polymer temperature at extrusion as shown in Figure 5-4. According to this figure, the more obvious reflection of PET crystals appeared for fibers had more

remarkable roughness.

5.3.2 Crystallization of PET Component of Rough and Smooth Surface co-PA/PET/PET Blend Fibers

It was reported in chapter 2 that the surface roughness can be developed even the major component is an amorphous polymer (see Figure 2-1). Considering that the crystallization of the minor component can be detected more easily if the major component does not crystallize, detailed structural analyses of the co-PA/PET fibers prepared with the extrusion temperatures of 235, 245 and 255 ^{o}C were carried out. WAXD patterns of co-PA/PET blend fibers are shown in Figure 5-5, in that the reflection of PET crystals for fiber spun with low extrusion temperature was seen quite clearly because the major component co-PA was amorphous. As shown in SEM photographs shown in Figure 5-6, the fibers prepared at the extrusion temperatures of 235 and 245 ^{o}C exhibited rough surface whereas the fiber prepared at 255 ^{o}C had smooth surface. Wide angle X-ray intensity distribution patterns of the co-PA/PET blend fibers prepared at extrusion temperatures of 235, 245 and 255 ^{o}C are also compared in Figure 5-6. Along with the amorphous halo, an obvious circular crystalline reflection was observed for the fibers spun at 235 and 245 ^{o}C. It is well known that amorphous PET fibers can be obtained in ordinary melt spinning process because of its low crystallization rate, and well-developed crystalline structure can be formed only with high take-up velocities where the concept of orientation induced crystallization is applicable [6-8]. In Figure 5-6, similar results as the one in Figure 5-3 can be obtained, i.e. more sufficient crystallization of PET occurred in the melt spinning of co-PA6/PET blend when the surface roughness is developed because of low extrusion temperature.

The crystalline state of PET in co-PA/PET fibers was also analyzed by the DSC. As same as PA6/PET fiber samples, the co-PA6/PET fiber samples were heated at a heating rate of 10 K/min up to 300 ^{o}C, and started to be cooled immediately after reaching the maximum temperature at a cooling rate of 40 K/min. According to Figure 5-7, although there was an influence of water adsorbed to co-PA, clear cold crystallization peak of PET

appeared at around 110 ^{o}C for smooth surface fiber spun with extrusion temperature of 255 ^{o}C. Meanwhile melting peak of PET component was observed at around 255 ^{o}C for the three samples. The melting peak temperature of the fiber prepared at 255 ^{o}C was slightly lower than the other two samples. Consulting the results of WAXD measurement shown in Figures 5-5 and 5-6, it is considered that the melting peak of the fiber spun at 255 ^{o}C contains the melting of crystals formed by the cold crystallization at around 110 ^{o}C during the heating process, whereas at least a part of crystals corresponding to the melting peak of fibers prepared at 235 and 245 ^{o}C are formed during the spinning processes.

If the cooling process started without holding time after the heating of samples up to 300 ^{o}C, clear exothermic peaks appeared in the DSC thermogram for the samples with low extrusion temperatures. This result indicates that high crystallizability was introduced to the PET component in the spinning process with low extrusion temperatures, and such high crystallizability remained even after its melting. To analyze the thermal stability of high crystallizability, effects of maximum temperature and holding time in the DSC measurement on the crystallization behavior of PET component in the cooling process were investigated. The DSC thermograms for the fibers prepared at 245 ^{o}C is summarized in Figure 5-8. It was found that the crystallization during the cooling process in the DSC measurement became less distinct with the increases of maximum temperature and holding time. These results suggest that 1) a “structure” of long relaxation time was developed in PET component in the co-PA/PET blend in the spinning process, 2) development of such “structure” caused the enhancement of the crystallization of PET component, and 3) the crystallization of PET eventually led to the development of surface roughness on the produced fibers. It should come into notice that such mechanism for the formation of fibers with surface roughness is applicable to various combinations of polymer blends as described in chapter 2. Strong memory effect of polymer melt after shear flow near or above the nominal melting temperature has been reported by Matsuba [9].

5.3.3 Effect of Temperatures of Barrel, Adapter, etc.

In melt spinning process, polymer blends flowed through barrel of twin screw extruder, spinning head, adapter, capillary1, capillary2, gear pump and spinneret one by one. In most melt spinning conditions, the barrel temperatures were fixed, only extrusion temperature which includes temperatures from spinning head to spinneret were changed. It should be noticed that temperature of C2 area of barrel was 260 ^{o}C higher than the melting temperature of PET and PA component. In this research, the temperature of each area from C3 to spinneret was increased one by one. With each temperature condition, fiber sample was collected, named as NO.1~NO.8. The SEM photographs of as-spun fiber samples of NO.1 ~ NO.8 are shown in Figure 5-13. In that, it can be seen roughness of fiber samples NO.7 and NO.8 were distinguished from other samples. That means the temperatures of gear pump and spinneret influenced the roughness obviously, in the other words, the roughness maybe formed just because of the low temperature of gear pump and spinneret which enhanced the crystallization of PET component. DSC thermograms of heating process are shown in Figure 5-10. Obvious cold crystallization of each fiber sample of NO.7, NO.8 can be observed. As same conclusion as it has been certified, cold crystallization of PET component appeared for fiber with smooth surface because of higher temperature. From SEM photographs of Figure 5-9, difference between NO.1~NO.6 was not clear. But for DSC thermograms, the cold crystallization of NO.1 and NO.2 samples did not appear. More sufficient crystallization happened in these two fiber samples. This result can also be certified in WAXD intensity distribution curves shown in Figure 5-11. The reflection of PET crystals at about diffraction angle of 26.1 ^{o} can be seen for fiber samples NO.1 and NO.2. Only for fiber samples NO.7 and NO.8, the (100) reflection from the triclinic crystal of PET at the diffraction angle of 26.1 degree disappeared. That means when the temperatures of gear pump and spinneret were kept at low values, the crystallization of PET component was enhanced even the temperatures of other areas were changed to quite high values.

As it has been introduced, enhanced PET crystals appeared for fibers with rough surface, also in chapter 2, it has been found that the crystallizability of minor component

is necessary for formation of roughness with blend of two kinds of polymers in melt spinning. Considering the above conclusions and the effect of temperature of barrel, adapter, etc. for crystallization of PET component and the degree of roughness shown in this chapter, it can be certified that, crystallization of PET component appeared in the area of gear pump and spinneret could take responsible for the formation of roughness in the melt spinning process with PA6/PET blends. Intensity of reflection of PET crystals and heat of cold crystallization PET of fiber samples NO.1~NO.8 are shown in Figure 5-12. Intensity of reflection of PET crystals decreased from NO.1 to NO.8, on the other hand, heat of cold crystallization increased.

5.3.4 Development of Roughness along the Spin-line

It has been found that roughness of fiber sample can be enhanced by low extrusion temperature. SEM photographs of fiber samples spun with various extrusion temperatures obtained at different positions from spin-line are shown in Figure 5-13. With high extrusion temperature of 265 ^{o}C, roughness can barely be seen at any distances from spinneret. With low extrusion temperature of 255, roughness appeared from the position closed to the spinneret. The same results had been introduced in chapter 3, see Figure 3-12.

5.3.5 Differentiation of PET Components in PA6/PET Blend Fibers

SEM photographs of fiber samples spun with different extrusion temperatures with a nozzle diameter of 0.5 mm are shown in Figure 5-14 (a.) (b.) (c.). After removing PET component by alkali treatment, the difference between fiber samples' surfaces is quite obvious as can be seen in Figures 5-14 (d.) (e.) (f.). With high extrusion temperature, PET component existed in the surface of PA6/PET blend fiber mostly. The existence of PET component of rough surface fiber spun with low extrusion temperature can barely be obtained. According to SEM photographs of fiber sample cross sections showing in Figures 5-14 (g.) (h.) (i.), obviously, the bright component existed inside of fiber spun with low extrusion temperature. Through analysis of energy dispersive X-ray detector

equipped in SEM2, it can be inferred that the bright part was PET component. That means the differentiation of PET component in blend fibers changed with various extrusion temperatures. With high extrusion temperature, in the cross section, the bright PET component decreased because it shifted to the surface of fiber. In addition, the axis sections of rough surface fiber were also analyzed by SEM2, see Figure 5-15. It has been certified that the PET component can barely be found on the surface of fibers with enhanced roughness. In the Figure 5-19, the bright parts which were recognized as PET component were existing inside of fibers, especially inside of the bulges. That means the PET component constituted the roughness of PA6/PET blend fibers even the bulges were covered by PA6 component. In the big bugles, it can be seen the PET component existed as several small parts and kept together. That structures maybe the reason for the PET crystallization which was very difficult to be melted and also could take responsible for the roughness of fibers produced by PA6/PET blends with melt spinning. According to the conclusion of 5.3.3, that structure may be formed in the spinneret during melt spinning because of low extrusion temperature.

5.4 Conclusions

For the PA6/PET blend fibers prepared with various spinning conditions, cold crystallization behavior of PET component was analyzed from the DSC thermogram, while crystalline state of PET component was also analyzed from the WAXD intensity analysis. The fibers with rough surface tend to exhibit crystalline reflection of PET in the WAXD diagram, while cold crystallization peak of PET was less distinct in the DSC thermogram. On the other hand, the fibers with smooth surface tend to exhibit distinct cold crystallization peak while crystalline reflection was less distinct. The negative correlation between the *R*a values and cold crystallization peak area as well as the positive correlation between the *R*a values and crystalline peak intensity were confirmed. On the other hand, it was also revealed that the PET component in the fibers with rough surface keeps its high crystallizability even after its melting. Through the analysis for the

differentiation of PET components in PA6/PET blend fibers, it was found that PET particles exist under the protruded part of rough fiber surface, while the surface is covered with PA6 component. These results strongly suggested that the crystallization of PET component in the spinning process is indispensable for the development of surface roughness, while the crystallizability of PET component was enhanced by the polymer flow especially near the spinneret.

Reference

[1] X.-S. Xu[1], Y. Shirakashi[2], J. Ishibashi[1], W. Takarada[1], T. Kikutani[1]. Evaluation of Surface Roughness Development of Blend Fibers through Fiber Diameter Measurement using Various Optical Equipments. 41st TEXTILE RESEARCH SYMPOSIUM

September 12-14, 2012, Guimar ães, Portugal.

[2] Shirakashi Y, Asakura O, Ito S, et al. Development of polyamide 6 based blend fibers with surface roughness for artificial hair. Seikei-Kakou 2011; 23: 358-364.

[3] Ziabicki A. Fundamentals of Fiber Formation. London: John Wiley & Sons, 1976, p.113.

[4] Daubeny R de D, Bunn CW, Brown CJ. The Crystal Structure of Polyethylene Terephthalate. Proc Roy Soc 1954; 226: 531-542.

[5] T. Kikutani. Y. Kawahara. T. Matsui, A. Takaku, and J. Shimizu, Seikei-Kako~, 1,333 (1989).

[6] Shimizu J, Okui N, Kikutani T. Fine Structure and Physical Properties of Fibers Melt-spun at High Speeds from Various Polymers in High-Speed Fiber Spinning. New York: John Wiley & Sons, 1985, p.429.

[7] Kikutani T, Nakao K, Takarada W, and Ito H. On-line measurement of orientation development in the high-speed melt spinning process. Polymer Engineering & Science 1999; 39: 2349–2357.

[8] Heuvel HM, Huisman R. Effect of winding speed on the physical structure of as-spun poly(ethylene terephthalate) fibers, including orientation-induced crystallization. Journal of Applied Polymer Science 1978; 22: 2229-2243.

[9] Matsuba G, Zhao Y, Nishida K, Kanaya T. Precursor of shish–kebab in isotactic polystyrene under shear flow. Polymer 2009; 50: 2095-2103.

Table 1. Conditions for melt spinning of blend fibers.

Polymers (80/20 wt%)	**Nozzle diameter (mm)**	**Barrel temperatures (^{o}C)**	**Extrusion Temperature (^{o}C)**	**Take-up velocity * (km/min)**	**Through-put rate (g/min)**
		C1 C2 C3 C4			
PA6/PET	2.0	160 260 235 235	255	0.27	5.8
			260		
			265		
	1.0		235		
			245		
			255		
	0.5		235		
			245		
			255		
			265	×	
co-PA/PET	1.0		235	0.124	
			245		
			255		

×: Fiber cannot be collected by roller.

*: Fibers spun with nozzle diameter of 1.0 mm, extrusion temperature of 250 ^{o}C were also taken-up with the take-up velocity of 1.0, 2.0, 3.0 and 4.0 km/min, respectively.

Table 2. Conditions for melt spinning of blend fibers with a nozzle diameter of 1.0 mm, through-put rate of 5.8 g/min and take-up velocity of 50 m/min.

	C1(°C)	C2(°C)	C3(°C)	C4(°C)	Spinning Head (°C)	Adapter (°C)	Capillary1 (°C)	Capillary2 (°C)	Gear Pump (°C)	Spinneret (°C)	Pressure (Pa)	R_a (μm)
NO. 1	160	260	235	235	245	245	245	245	245	245	7.2	5.4
NO. 2	160	260	260	235	245	245	245	245	245	245	7.0	5.2
NO.3	160	260	260	260	245	245	245	245	245	245	6.2	7.1
NO.4	160	260	260	260	260	260	245	245	245	245	6.2	3.0
NO.5	160	260	260	260	260	260	260	245	245	245	5.6	3.6
NO.6	160	260	260	260	260	260	260	260	245	245	5.5	3.8
NO.7	160	260	260	260	260	260	260	260	260	245	4.0	1.8
NO.8	160	260	260	260	260	260	260	260	260	260	3.0	1.3

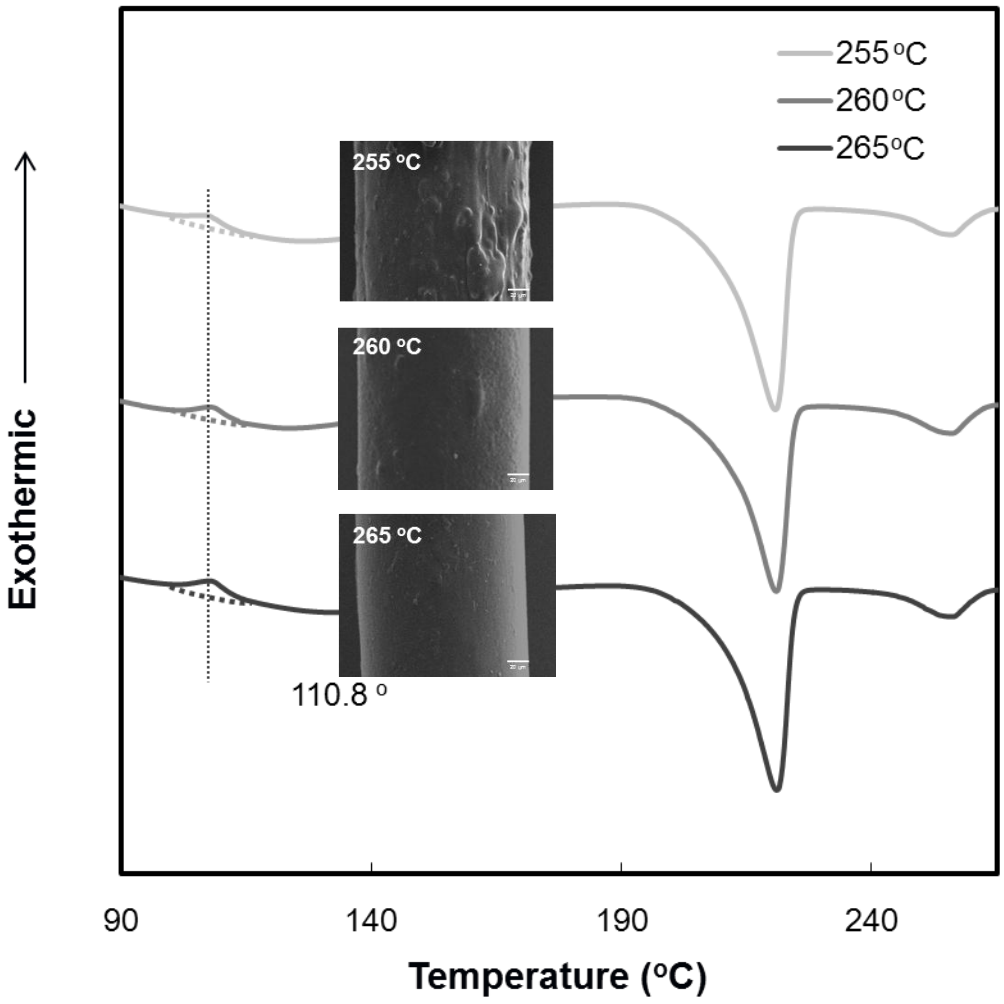

Figure 5-1. SEM1 photo graphs and DSC thermograms obtained during heating processes of PA6/PET blend fibers melt spun with different extrusion temperatures of 255, 260, 265 °C, with a nozzle diameter of 2.0 mm, through-put rate of 5.8 g/min, take-up velocity of 0.27 km/min. Areas between dotted line and full line of fibers melt spun with different nozzle diameters and extrusion temperatures were compared in next figure.

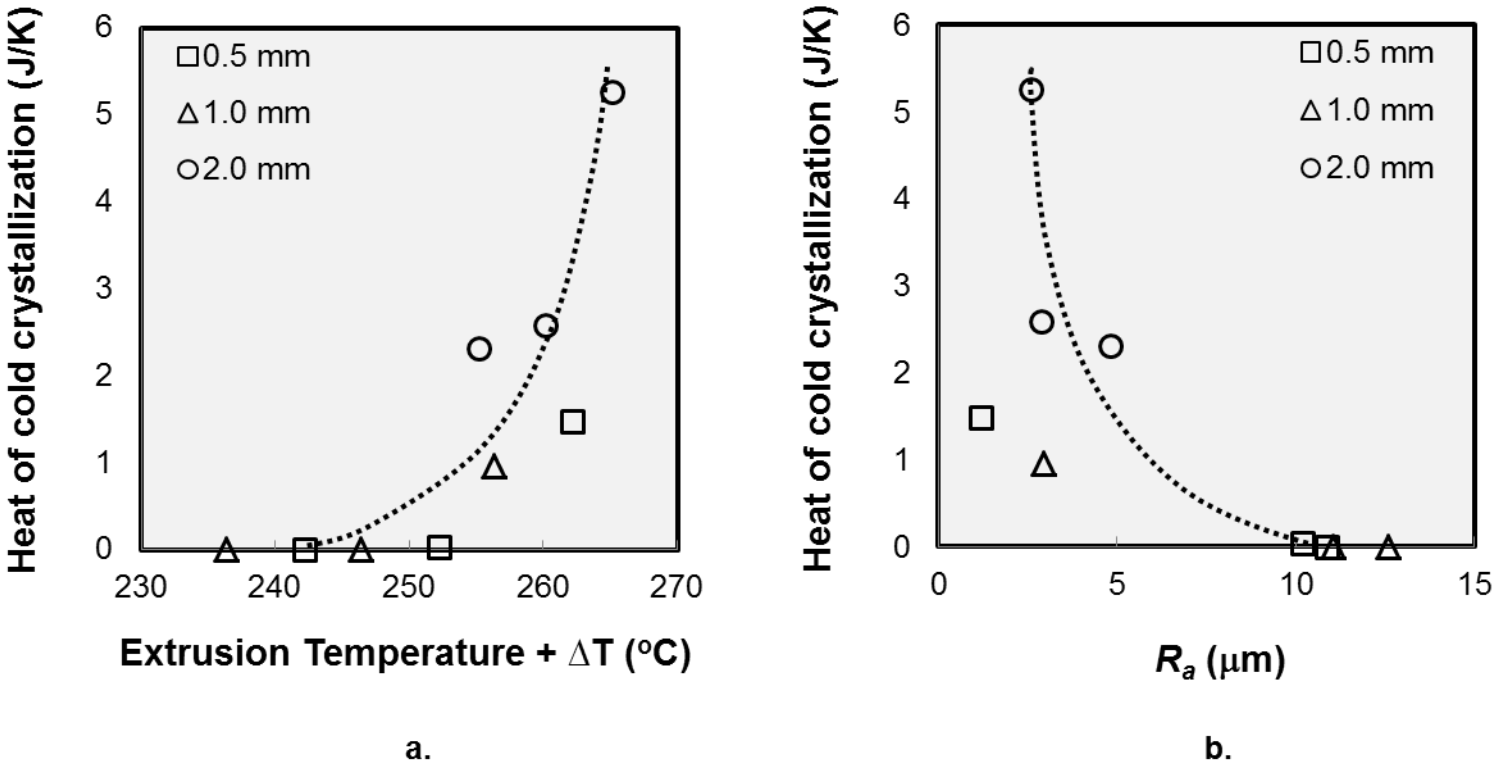

Figure 5-2. (a.) DSC thermograms obtained during heating processes for PA6/PET blend fibers melt spun with different polymer temperatures in the various nozzlezs with diameters of 0.5, 1.0 and 2.0 mm, with a through-put rate of 5.8 g/min, take-up velocity of 0.27 km/min. (b.) Relationship between DSC thermograms obtained during heating processes and R_a values of PA6/PET1 blend fibers melt spun with different polymer temperatures in the various nozzles with diameters of 0.5, 1.0 and 2.0 mm, with through-put rate of 5.8 g/min, take-up velocity of 0.27 km/min.

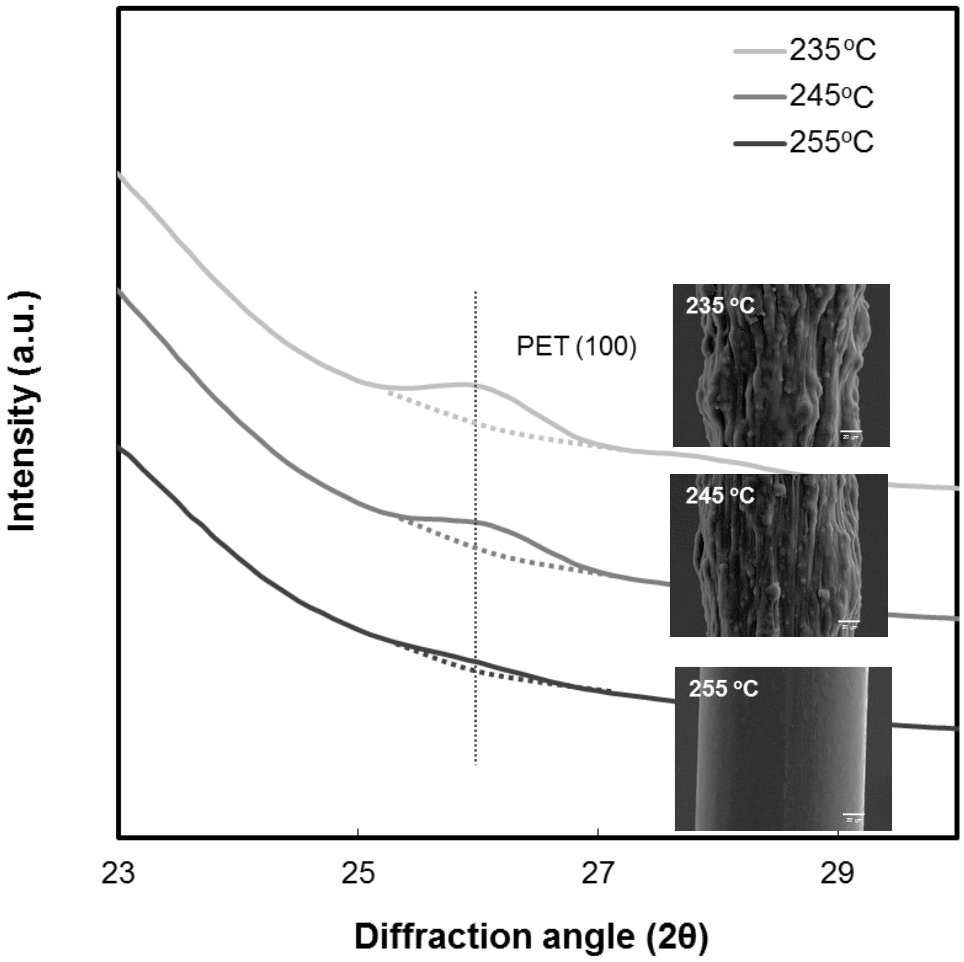

Figure 5-3. SEM1 photo graphs and WAXD intensity distribution curves for PA6/PET blend fibers melt spun with different extrusion temperatures of 235, 245, 255 ^{o}C, with a nozzle diameter of 1.0 mm, through-put rate of 5.8 g/min, take-up velocity of 0.27 km/min. Areas between dotted line and full line of fibers melt spun with different nozzle diameters and extrusion temperatures were compared in next figure.

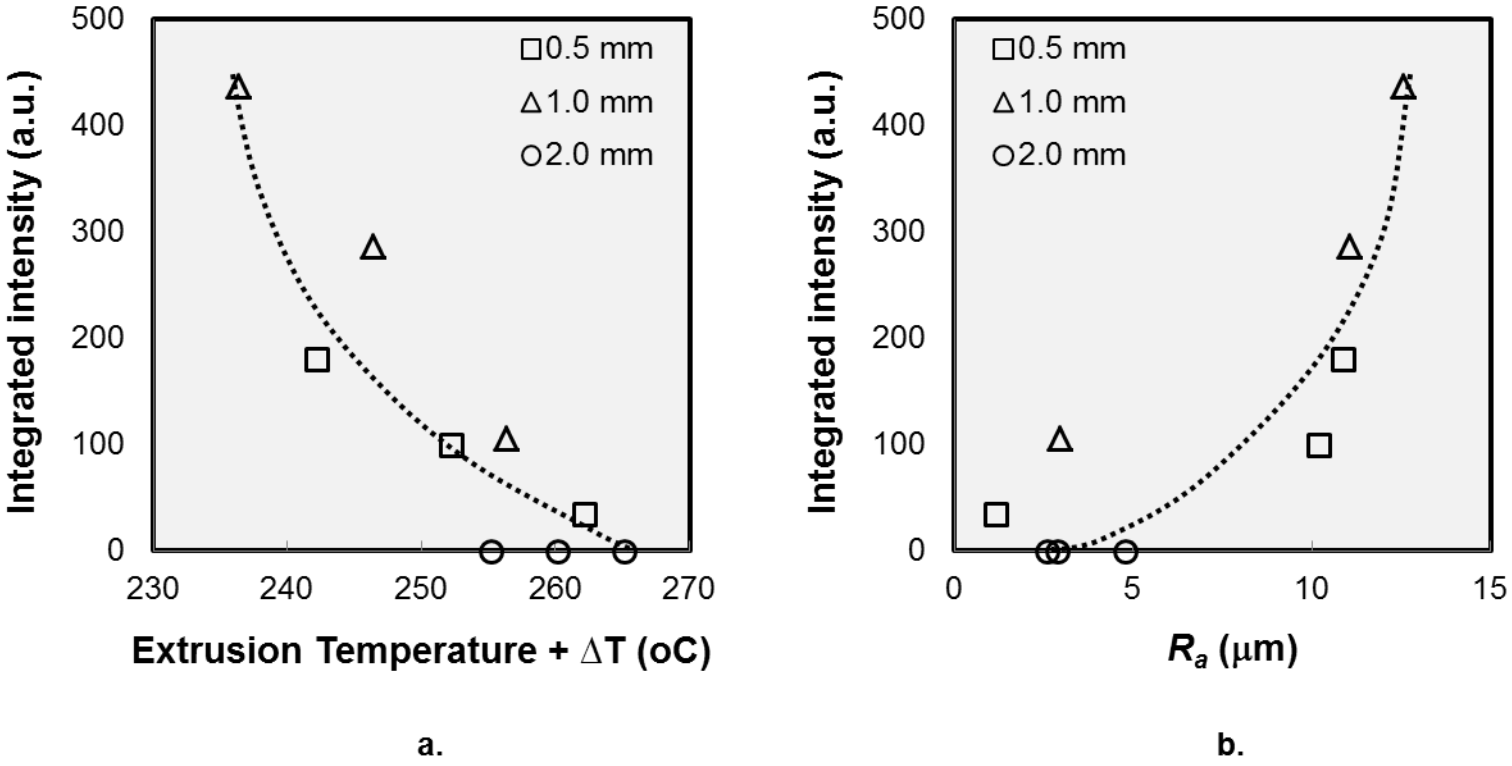

Figure 5-4. (a.) WAXD intensity for PA6/PET blend fibers melt spun with different polymer temperatures in the various nozzles with diameters of 0.5, 1.0 and 2.0 mm, with a through-put rate of 5.8 g/min, take-up velocity of 0.27 km/min. (b.) Relationship between WAXD intensity and R_a values of PA6/PET blend fibers melt spun with different polymer temperatures in the various nozzles with diameters of 0.5, 1.0 and 2.0 mm, with through-put rate of 5.8 g/min, take-up velocity of 0.27 km/min.

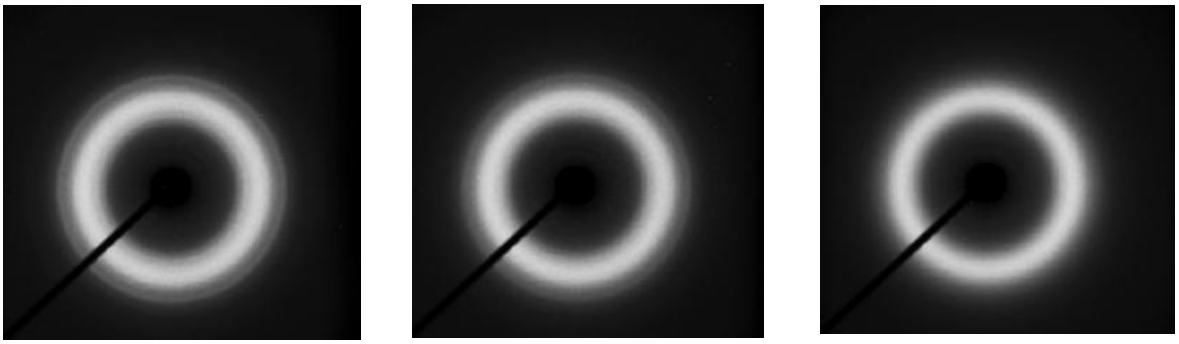

235 °C **245 °C** **255 °C**

Figure 5-5. WAXD patterns of as spun co-PA/PET fibers melt spun with different extrusion temperatures of 235, 245 and 255 °C. Through-put rate 5.8 g/min, nozzle diameter 1.0 mm, take-up velocity 0.124 m/min.

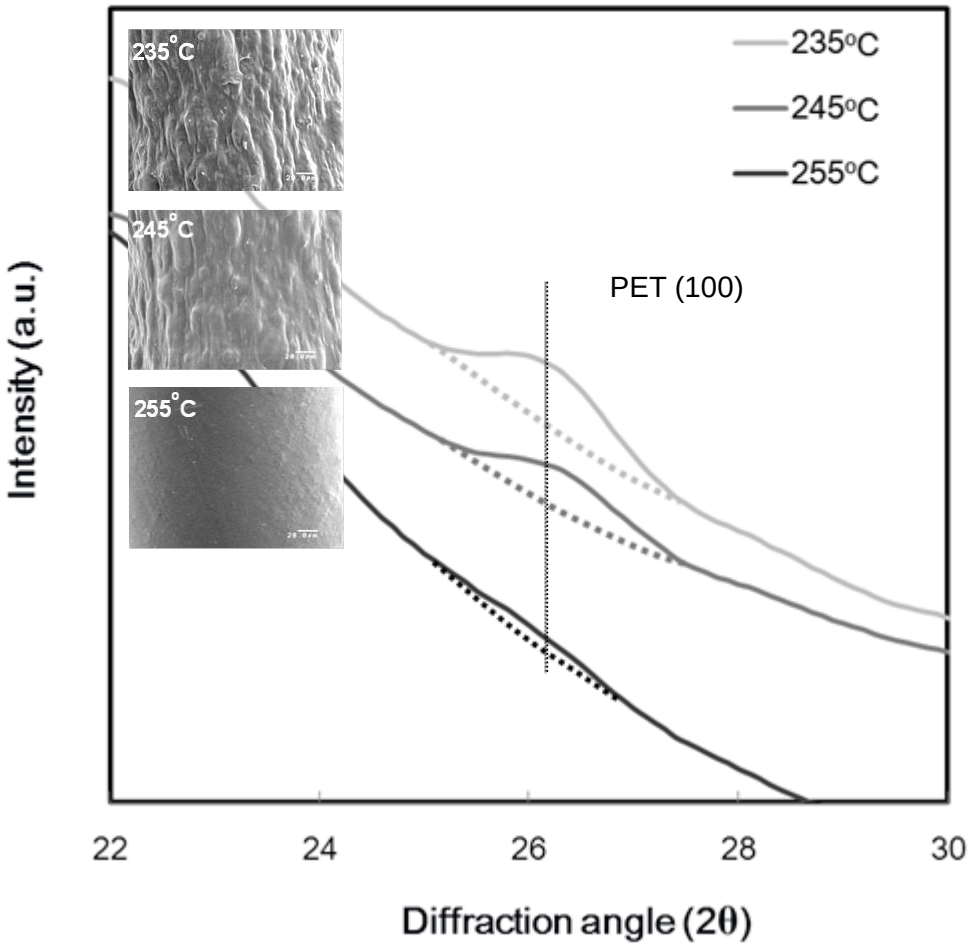

Figure 5-6. SEM1 photographs and WAXD intensity distribution curves for co-PA/PET fibers melt spun with different extrusion temperatures of 235, 245 and 255 ^{o}C. Through-put rate 5.8 g/min, nozzle diameter 1.0 mm, take-up velocity 0.124 km/min.

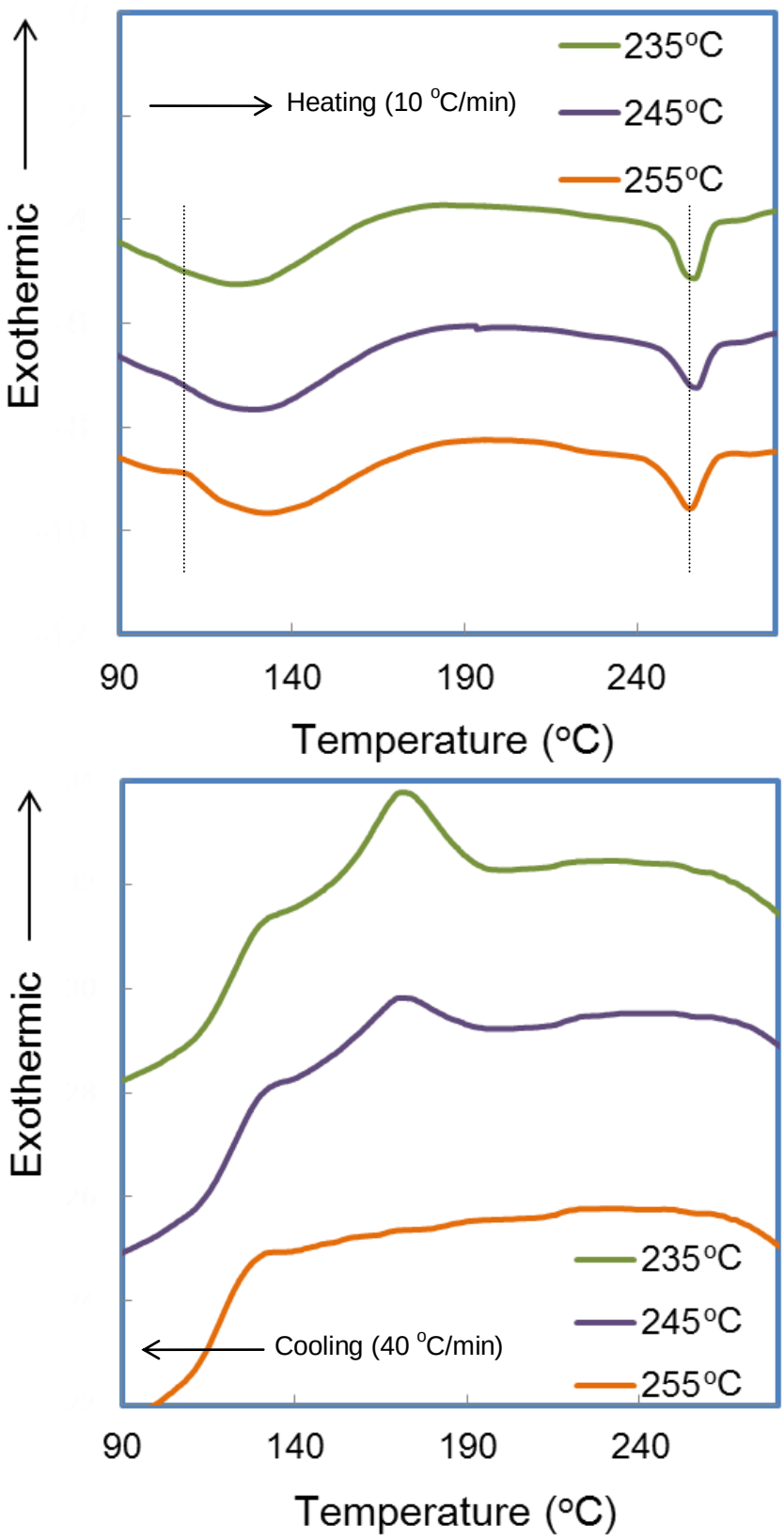

Figure 5-7. DSC thermograms obtained during heating and cooling processes of co-PA/PET (80/20 wt%) fibers melt spun with different extrusion temperatures of 235, 245 and 255 °C. Through-put rate 5.8 g/min, nozzle diameter 1.0 mm, take-up velocity 0.124 m/min.

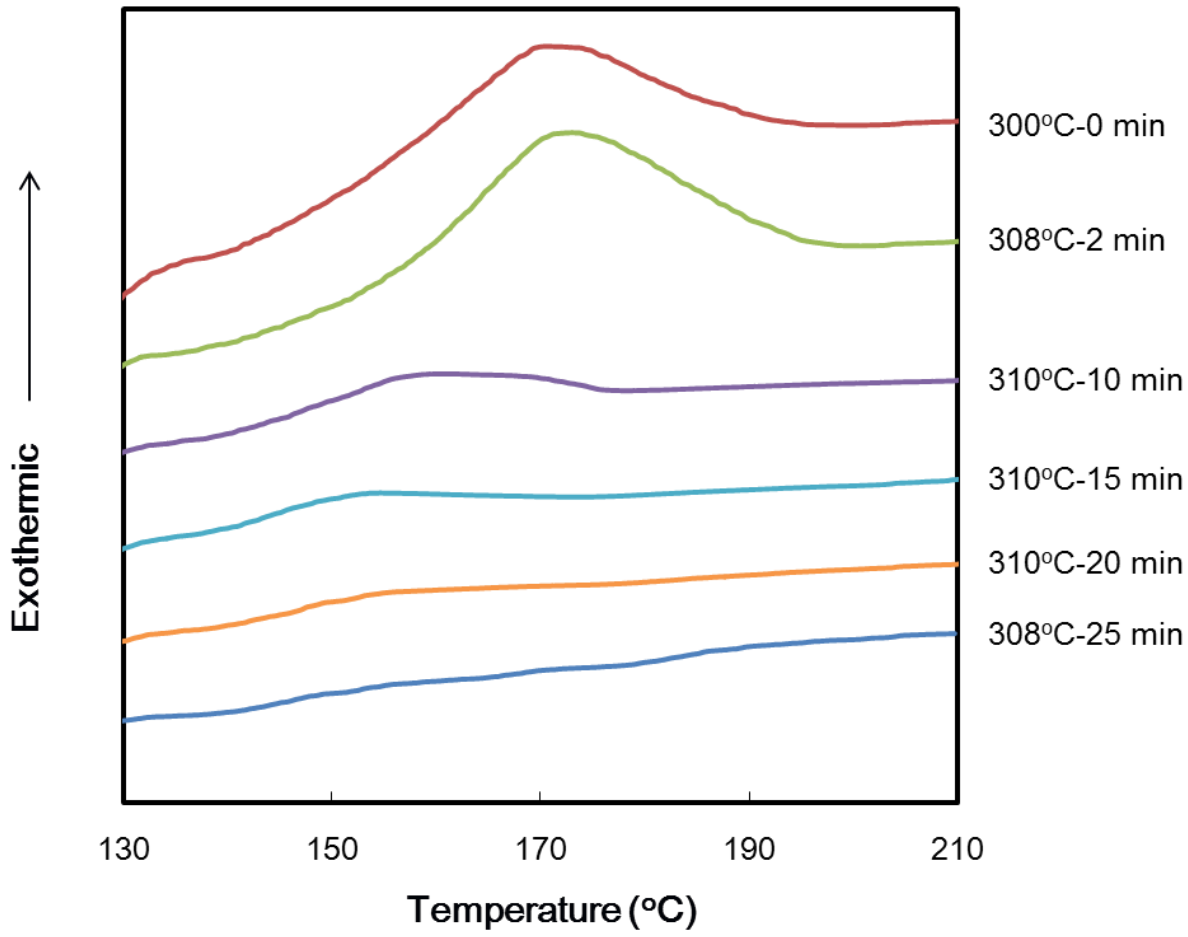

Figure 5-8. DSC thermograms obtained during cooling process of co-PA/PET (80/20 wt%) fibers melt spun with an extrusion temperatures of 245 °C. Through-put rate 5.8 g/min, nozzle diameter 1.0 mm, take-up velocity 0.124 m/min. Different maximum temperatures and holding times were applied to the sample before the starting of measurements are indicated in the figure.

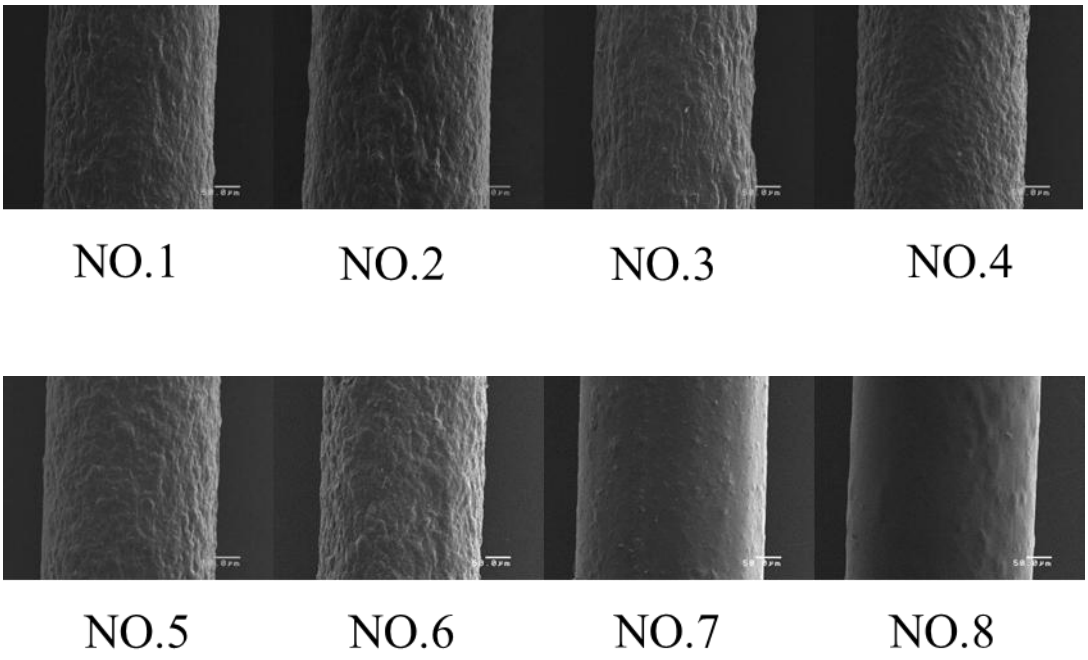

Figure 5-9. SEM1 photographs of PA6/PET blend fibers melt spun with different barrel and extrusion temperatures, with a nozzle diameter of 1.0 mm, through-put rate of 5.8 g/min and take-up velocity of 0.05 km/min.

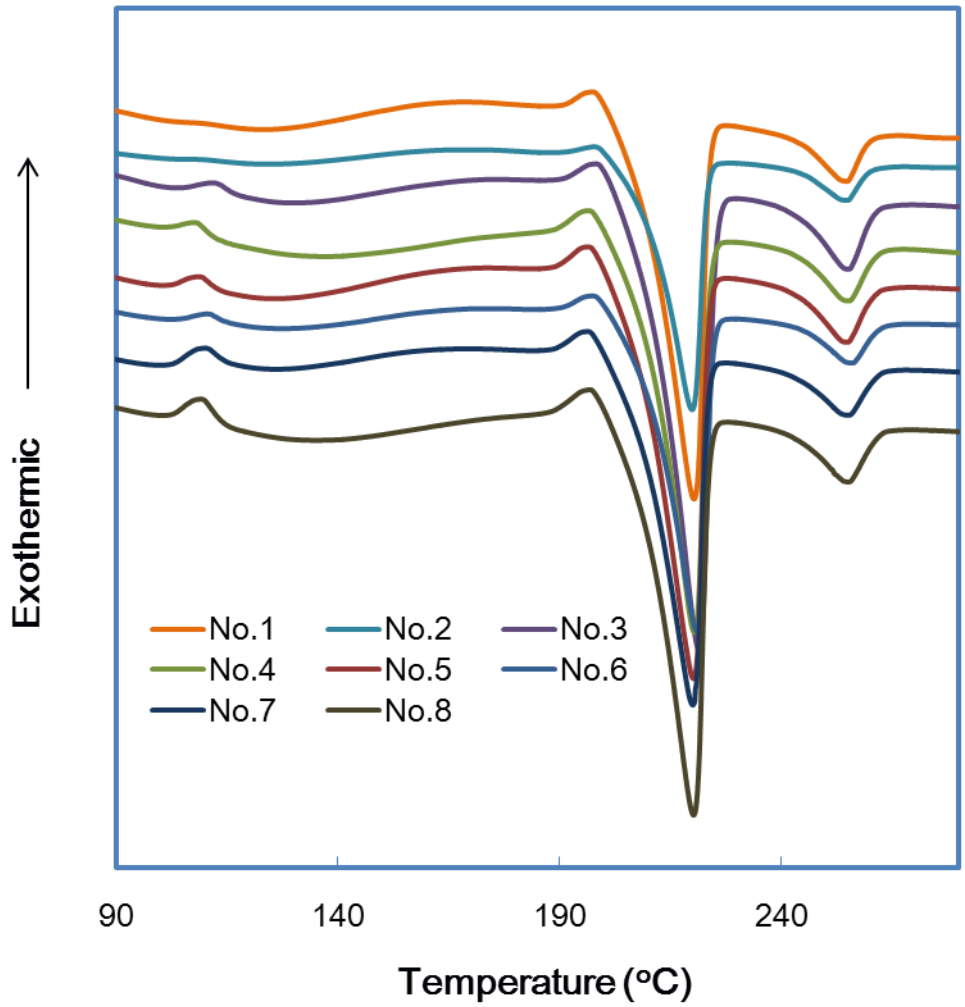

Figure 5-10. DSC thermograms obtained during heating processes of PA6/PET blend fibers melt spun with different barrel and extrusion temperatures, with a nozzle diameter of 1.0 mm, through-put rate of 5.8 g/min, and take-up velocity of 0.05 km/min.

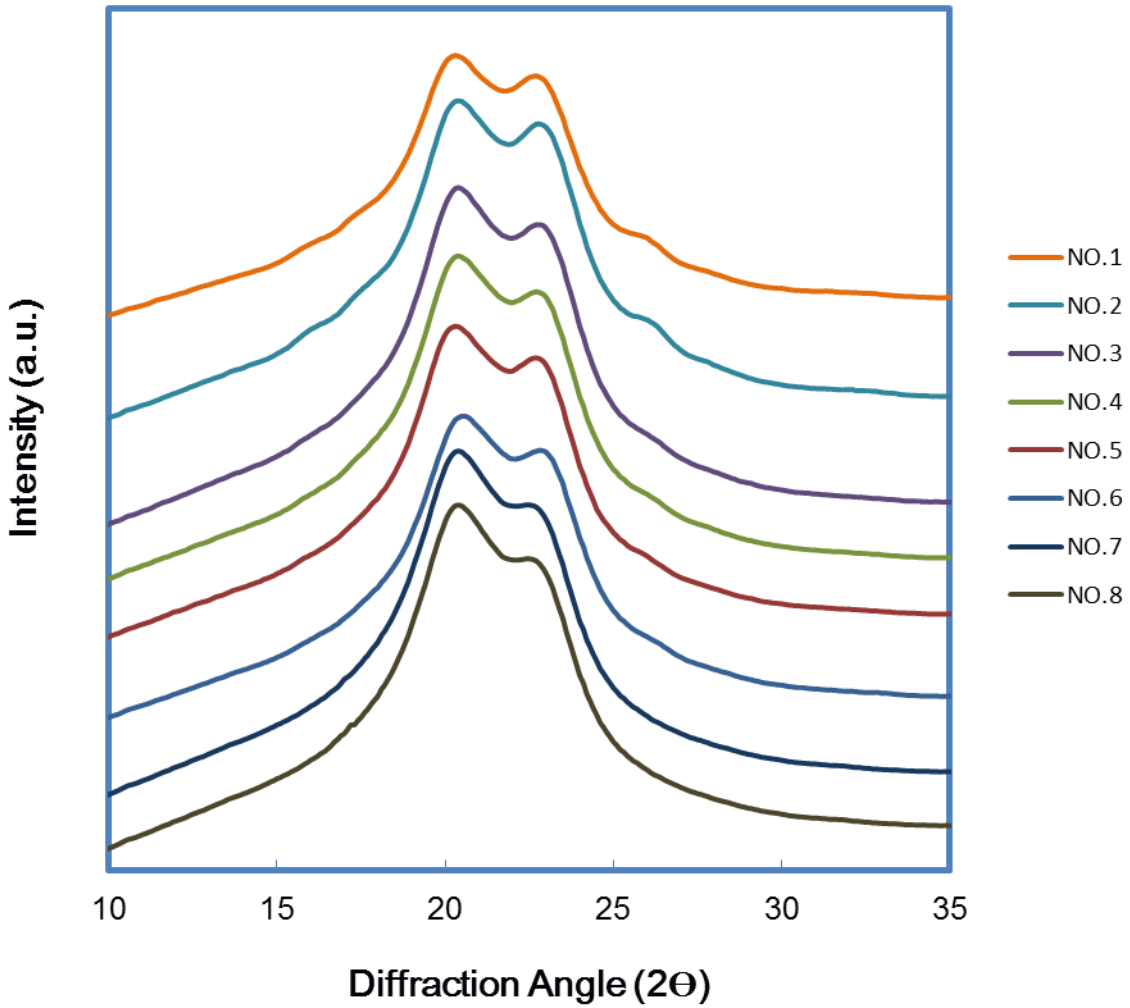

Figure 5-11. WAXD intensity distribution curves for PA6/PET blend fibers melt spun with different barrel and extrusion temperatures, with a nozzle diameter of 1.0 mm, through-put rate of 5.8 g/min, and take-up velocity of 0.05 km/min.

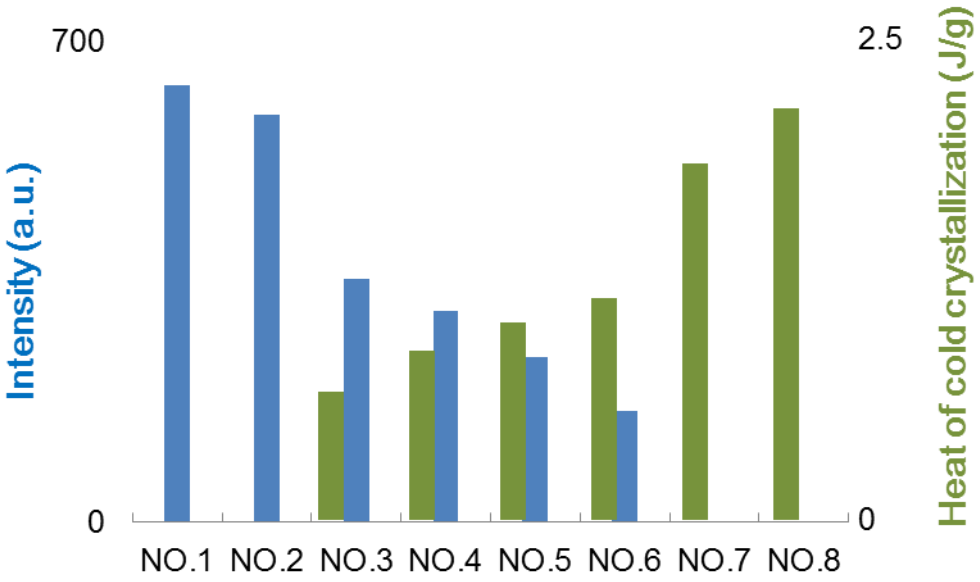

Figure 5-12. Results of WAXD and DSC thermograms for PA6/PET blend fibers melt spun with different barrel and extrusion temperatures, with a nozzle diameter of 1.0 mm, through-put rate of 5.8 g/min, and take-up velocity of 0.05 km/min.

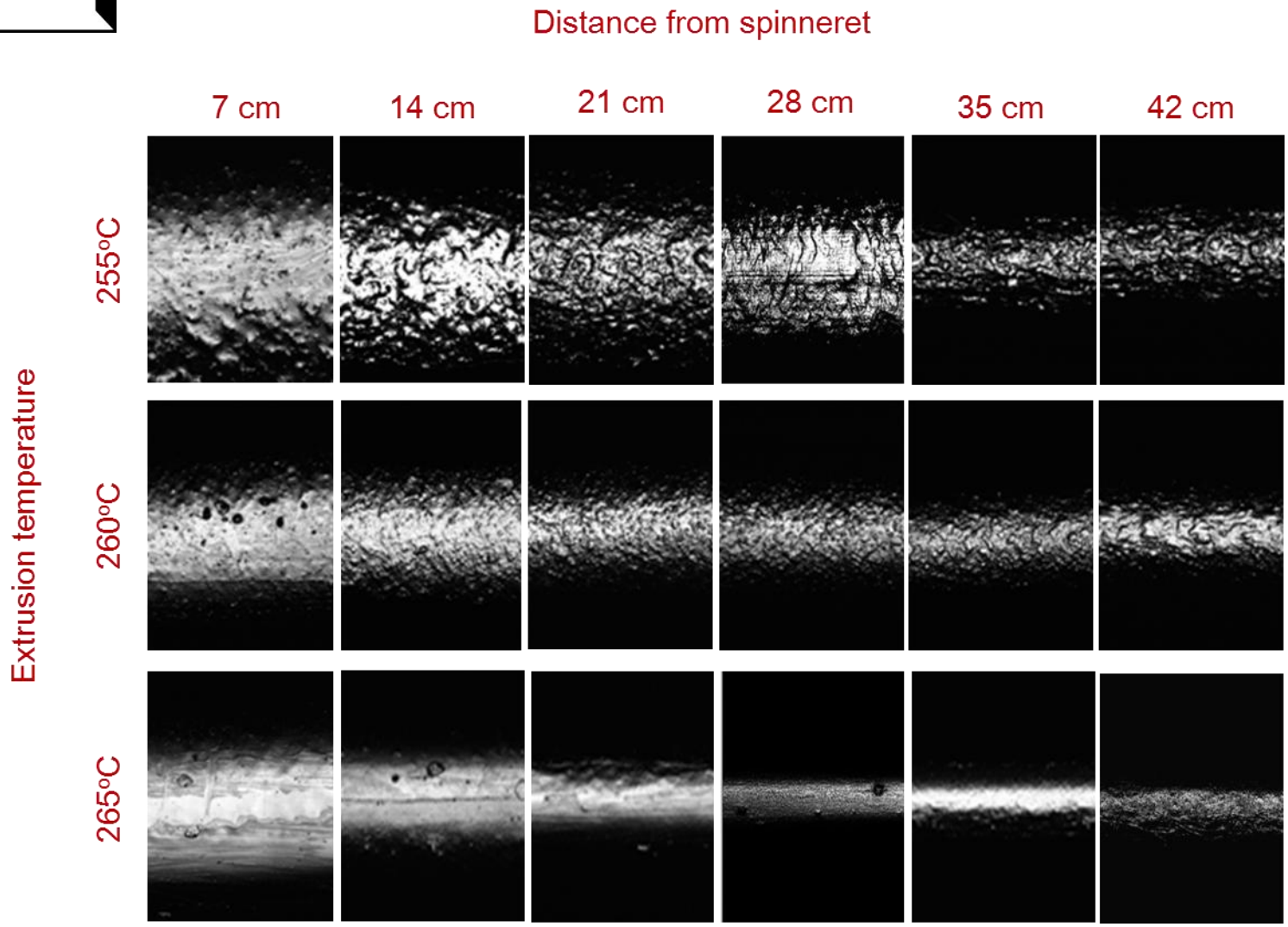

Figure 5-13. Development of roughness of free-fall PA6/PET blend fibers melt spun with different extrusion temperatures, 255, 260 and 265 °C took by LM, through-put rate, nozzle diameter are 5.8 g/min and 2.0 mm, respectively.

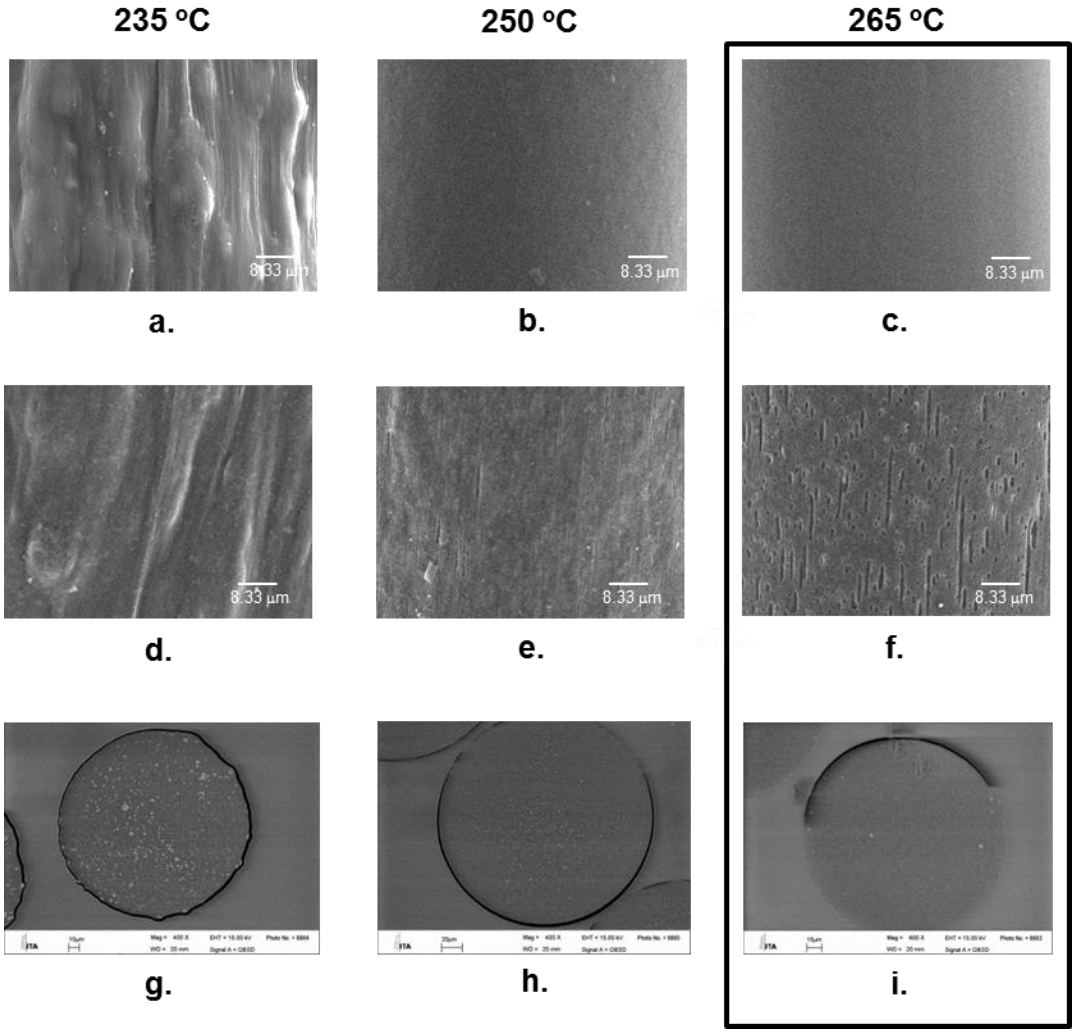

Figure 5-14. (a.) (b.) (c.): SEM1 photographs of blend fibers melt spun with different extrusion temperatures of 235, 250 and 265 ^{o}C, with a nozzle diameter of 0.5 mm, through-put rate of 5.8 g/min and take-up velocity of 0.27 m/min. (d.) (e.) (f.): SEM1 photographs of surface of fibers shown in (a.) (b.) (c.) treated by sodium hydroxide solution (20 wt%) at 100 ^{o}C for 1 hour. (g.) (h.) (i.): SEM2 photographs of cross-section of fibers shown in (a.) (b.) (c.) . Fibers in the black frame cannot be taken by roller.

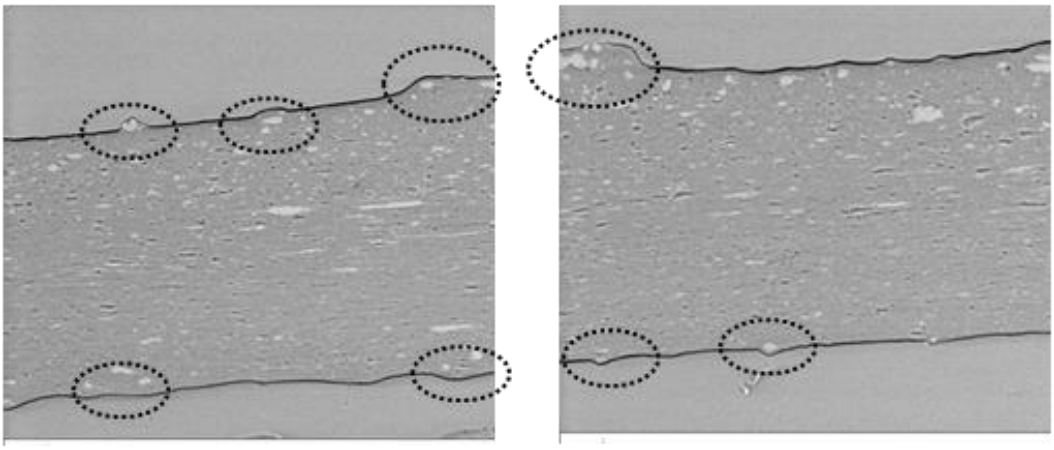

Figure 5-15. SEM photographs of axis sections of PA6/PET blend fibers melt spun with an extrusion temperatures of 255 ^{o}C, nozzle diameter of 20 mm, through-put rate of 5.8 g/min and take-up velocity of 0.27 m/min

Chapter 6

General Conclusions

Chapter 6
General Conclusions

In this thesis, mechanism of surface roughness development in the newly developed technology for the production of fibers for artificial hair was investigated. In the production of fibers for artificial hair, control of surface roughness is indispensable for achieving good appearances.

Chapter 1 is the general introduction of this thesis. It was stated that incorporation of surface roughness is necessary in the production of fibers for artificial hair since human hair as well as hair of any animal exhibits surface roughness. Various technologies developed in the artificial hair industry for producing synthetic fibers with surface roughness was introduced.

In chapter 2, to elucidate the necessary conditions for the development of roughness on the surface of blend fibers, melt spinning of various combinations of blend polymers were carried out under a wide-range of spinning conditions. It was concluded that the necessary conditions for the formation of surface roughness are: (1) the minor component is a crystalline polymer, (2) the major component is melt processable at a temperature lower than the melting temperature of the minor component and (3) extrusion temperature is lower than the melting temperature of the minor component.

In Chapter 3, three kinds of optical equipment were applied for the quantitative evaluation of surface roughness of PA6/PET blend fibers with and without roughness. In this research, optical microscope, scanning electron microscope and edge-detection type diameter monitor (EDDM) were applied for off-line evaluation of the surface roughness, while back-illumination type diameter monitor (BIDM) was applied for on-line measurement of surface roughness development in the melt spinning process. Optimum method of data analysis for evaluation of parameter R_a which stands for the degree of roughness was investigated. There was a fairly high correlation between the R_a values obtained from the off-line measurement of as-spun fibers using the EDDM and those from the on-line measurement of the spin-line using the BIDM. Utilizing such correlation,

it was revealed that the roughness develops gradually with the increase of distance from the spinneret in the spinning process.

In chapter 4, effects of several processing parameters in melt spinning process on the development of surface roughness were investigated. Surface roughness can be enhanced when extrusion temperature was lowered. Smaller nozzle diameter could lead to the increase of the true temperature of polymer blends in the spinning nozzle. Accordingly, the fibers produced using a nozzle of larger diameter showed higher degree of surface roughness at the same extrusion temperature. On the other hand, because of the combination of spinnability and extrusion temperature, the most developed roughness appeared for the fiber produced with the nozzle diameter of 1.0 mm. The larger through-put rate and lower take-up velocity also lead to the increase in the R_a values of PA6/PET blend fibers, while the R_a/D values, the degree of roughness standardized by the fiber diameter, increased at the lower through put rate and higher take-up velocity where thinner fibers were produced. Lastly, incorporation of the water bath in the spin-line and the use of PET with higher intrinsic viscosity were found to cause the decrease of surface roughness.

In chapter 5, for the PA6/PET blend fibers prepared with various spinning conditions, cold crystallization behavior of PET component was analyzed from the DSC thermogram, while crystalline state of PET component was also analyzed from the WAXD intensity analysis. The fibers with rough surface tend to exhibit crystalline reflection of PET in the WAXD diagram, while cold crystallization peak of PET was less distinct in the DSC thermogram. On the other hand, the fibers with smooth surface tend to exhibit distinct cold crystallization peak while crystalline reflection was less distinct. The negative correlation between the *R*a values and cold crystallization peak area as well as the positive correlation between the *R*a values and crystalline peak intensity were confirmed. On the other hand, it was also revealed that the PET component in the fibers with rough surface keeps its high crystallizability even after its melting. Through the analysis for the differentiation of PET components in PA6/PET blend fibers, it was found that PET particles exist under the protruded part of rough fiber surface, while the surface is

covered with PA6 component. These results strongly suggested that the crystallization of PET component in the spinning process is indispensable for the development of surface roughness, while the crystallizability of PET component was enhanced by the polymer flow especially near the spinneret.

List of Publication

Mechanism of surface roughness development in melt spinning of blend fibers for artificial hair

Xu X, Shirakashi Y, Ishibashi J, Takarada W, Kikutani T

Submitted to Text Research Journal, 82(13), 1382-1389 (2012)

Evaluation of surface roughness development of polyamide 6/poly(ethylene terephthalate) blend fibers through fiber diameter measurement using three types of optical equipment

Xu X, Shirakashi Y, Ishibashi J, Takarada W, Kikutani T

Submitted to Text Research Journal,

Influence of spinning conditions on surface roughness development in melt spinning of blend fibers for artificial hair

Xu X, Shirakashi Y, Ishibashi J, Takarada W, Kikutani T

To be submitted

Influence of temperatures of barrels and spinneret in melt spinning for formation of rough surface fibers

Xu X, Shirakashi Y, Ishibashi J, Takarada W, Kikutani T

In preparing

Polyamide 6 Based Blend Fibers with Surface Roughness for Artificial Hair

Y. Shirakashi, O. Asakura, S. Ito, J. Ishibashi, X. Xu, W. Takarada, T. Kikutani

Seikei-Kakou, 23, 358-364 (2011)

Scientific Presentation

International conferences

Analysis on the Development of Surface Roughness in Melt Spinning of Fibers for Artificial Hair: Influence of extrusion temperature in melt spinning for rough surface fiber

X.-S. Xu[1], Y. Shirakashi[2], J. Ishibashi[1], W. Takarada[1], T. Kikutani[1]

ATC-10th,The 10th Asian Textile Conference

September 7-9, 2009, Ueda, Nagano, Japan

Mechanism of surface roughness development in melt spinning of blend fibers: Development process of roughness on the surface of PA6/PET blend fiber

X.-S. Xu[1], Y. Shirakashi[2], J. Ishibashi[1], W. Takarada[1], T. Kikutani

PPS-26th, the 26th Program and Abstracts

October 20-24, 2010, Istanbul, TURKEY

Analysis on the Development of Surface Roughness in Melt Spinning of Fibers for Artificial Hair: Distribution of PA6 and PET component in blend fiber

X.-S. Xu[1], Y. Shirakashi[2], J. Ishibashi[1], W. Takarada[1], T. Kikutani

Advanced Polymeric Materials and Technology Symposium

January 24-27, 2010, Shilla Hotel, Jeju, KOREA

Surface Roughness Development in Melt Spinning of Polymer Blends of Crystalline and Amorphous Polymers

X.-S. Xu[1], Y. Shirakashi[2], J. Ishibashi[1], W. Takarada[1], T. Kikutani[1]

Asian Workshop on Polymer Processing (AWPP2011 in China)
September 4~7, 2011, Qingdao, China

Mechanism of surface roughness development in melt spinning of blend fibers for artificial hair: Influence of nozzle diameter in melt spinning for rough surface fiber

X.-S. Xu[1], Y. Shirakashi[2], J. Ishibashi[1], W. Takarada[1], T. Kikutani[1]

International Symposium on New Frontiers in Fiber Materials Science
October 11-13, 2011, South Carolina, America

Mechanism of Surface Roughness Development in Melt Spinning of Blend Fibers for Artificial Hair: Influence of take-up velocity and through-put rate in melt spinning for rough surface fiber

X.-S. Xu[1], Y. Shirakashi[2], J. Ishibashi[1], W. Takarada[1], T. Kikutani[1]

Tokyo Tech-Tsinghua University Joint Symposium
November 16-19, 2011, Jingdezheng, China

MECHANISM OF SURFACE ROUGHNESS DEVELOPMENT IN MELT SPINNING OF BLEND FIBERS FOR ARTIFICIAL HAIR: CRYSTALLIZATION OF PET COMPONENT IN CO-PA/PET BLEND FIBER

X.-S. Xu[1], Y. Shirakashi[2], J. Ishibashi[1], W. Takarada[1], T. Kikutani[1]

Tokyo Tech-EPFL Joint Workshop

January 30 – February 3, 2012, Hakone-machi, Japan

Evaluation of Surface Roughness Development of Blend Fibers through Fiber Diameter Measurement using Various Optical Equipments

X.-S. Xu[1], Y. Shirakashi[2], J. Ishibashi[1], W. Takarada[1], T. Kikutani[1]

41st TEXTILE RESEARCH SYMPOSIUM

September 12-14, 2012, Guimarães, Portugal

Other conference

Analysis on the Development of Surface Roughness in Melt Spinning of Fibers for Artificial Hair: New method for producing of rough surface synthetic fibers

X.-S. Xu[1], Y. Shirakashi[2], J. Ishibashi[1], W. Takarada[1], T. Kikutani[1]

Japan Society of Polymer Processing ´09 Symposium

June 3~4, 2009, Tokyo, Japan

Analysis on the Development of Surface Roughness in Melt Spinning of Fibers for Artificial Hair: Universal rules for development of surface roughness through melt spinning with two kinds of polymers

X.-S. Xu[1], Y. Shirakashi[2], J. Ishibashi[1], W. Takarada[1], T. Kikutani[1]

Japan Society of Polymer Processing ´10 Symposium

June 1~2, 2010, Tokyo, Japan

Mechanism of Surface Roughness Development in Melt Spinning of Blend Fibers for Artificial Hair: Crystals of PET component in blend fibers

X.-S. Xu[1], Y. Shirakashi[2], J. Ishibashi[1], W. Takarada[1], T. Kikutani[1]

Autumn Meeting of the Society of Fiber Science and Technology, Japan

September 27~28, 2010, Yamakata, Japan

Evaluation of Surface Roughness Development of Blend Fibers through Fiber Diameter Measurement using Various Optical Equipments

X.-S. Xu[1], Y. Shirakashi[2], J. Ishibashi[1], W. Takarada[1], T. Kikutani[1]

The textile machinery society of Japan

June 1-2, 2012, Oosaka, Japan

EVALUATION OF SURFACE ROUGHNESS DEVELOPMENT OF BLEND FIBERS THROUGH FIBER DIAMETER MEASUREMENT USING VARIOUS OPTICAL EQUIPMENTS

X.-S. Xu[1], Y. Shirakashi[2], J. Ishibashi[1], W. Takarada[1], T. Kikutani[1]

第 43 回繊維学会夏季セミナー

August 8-10, 2012, Nara, Japan